Supporting Information

A Stable Heroin Analog That Can Serve as a Vaccine Hapten to Induce Antibodies that Block the Effects of Heroin and its Metabolites in Rodents and that Cross-React Immunologically with Related Drugs of Abuse

Agnieszka Sulima,[†] Rashmi Jalah,[§,#] Joshua F. G. Antoline,[†] Oscar B. Torres, [§,#] Gregory H. Imler,[‡] Jeffrey R. Deschamps,[‡] Zoltan Beck,[§,#] Carl R. Alving,[§] Arthur E. Jacobson,[†] Kenner C. Rice[†,]*, Gary R. Matyas,[#]*

[†]Drug Design and Synthesis Section, Molecular Targets and Medications Discovery Branch, Intramural Research Program, National Institute on Drug Abuse and the National Institute on Alcohol Abuse and Alcoholism, National Institutes of Health, Department of Health and Human Services, 9800 Medical Center Drive, Bethesda, MD 20892-3373, United States

[‡]Center for Biomolecular Science and Engineering, Naval Research Laboratory, Washington DC 20375, United States

[§]U.S. Military HIV Research Program, [#] Henry M. Jackson Foundation for the Advancement of Military Medicine, Walter Reed Army Institute of Research, 6720A Rockledge Drive, Bethesda, MD 20817, United States

[#] U.S. Military HIV Research Program, Walter Reed Army Institute of Research, 503 Robert Grant Avenue, Silver Spring, MD 20910, United States

*Corresponding authors

Contents

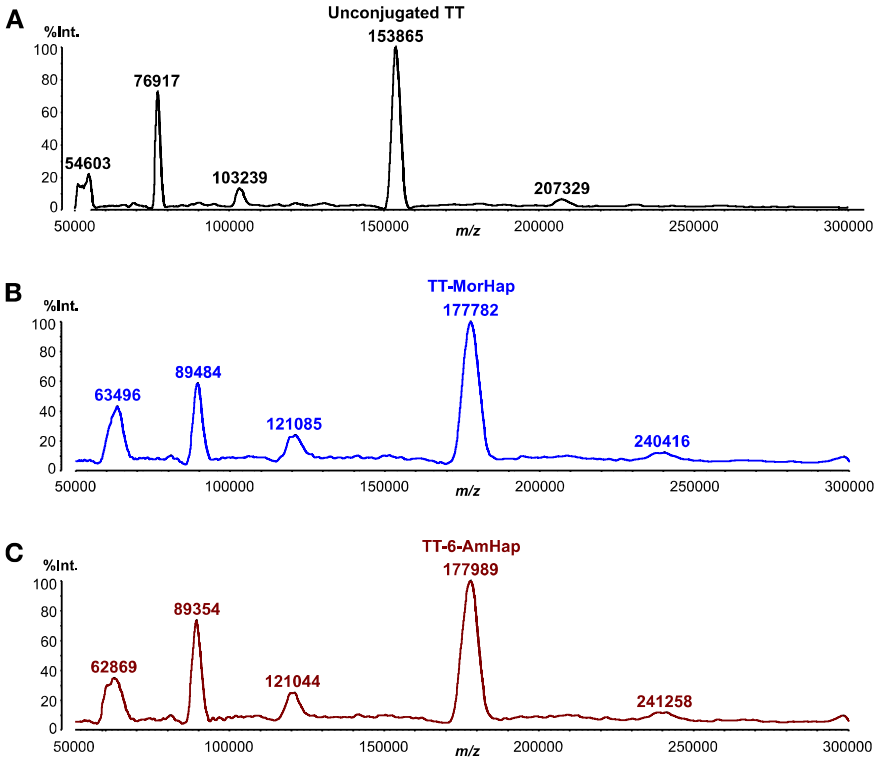

Figure S1. MALDI-TOF MS spectra of heroin vaccine bioconjugates. The Matrix-Assisted Laser Desorption Ionization Time-of-Flight Mass Spectroscopy (MALDI-TOF MS) spectra of unconjugated tetanus toxoid carrier protein (A; TT; top black panel), TT-**3** (MorHap) (B; middle blue panel) and TT-**1** (6-AmHap) (C; bottom maroon panel) conjugates are shown. MALDI-TOF MS was performed using the Axima MegaTOF™ instrument (Shimadzu Scientific Instruments, Columbia, MD), as described before.[1-3] Briefly, TT and the TT-hapten conjugates generated using 1:1600 ratio of TT to (SM-$(PEG)_2$ linker were desalted using C_4 ZipTip (Millipore), mixed and spotted with sinapinic acid matrix (Sigma) and the mass spectra were acquired. The instrument was calibrated using IgG (Sigma) as standard. The average of 500 mass profiles in the linear mode were taken, smoothed using Gaussian method and mass assignments were done using threshold apex peak detection.

For the unconjugated TT (A), various peaks corresponding to the TT light chain (55 kDa, m/z), the doubly charged ion (77 kDa), the TT heavy chain (103 kDa), the TT monomer (major peak; 154 kDa), TT heavy chain dimer (207 kDa) and the TT dimer (307 kDa, not shown) were observed. Subsequent increases in mol. wt. were observed for all the TT forms in the TT-hapten conjugates. The differences in mol. wt. of the major peak (~154 kDa) were used to calculate the number of haptens attached to TT using the expression:

$$Number\ of\ haptens = \frac{Mass_{TT-hapten\ conjugate} - Mass_{TT\ carrier\ protein}}{Mass_{hapten-linker}}$$

$Mass_{MorHap-linker}$ and $Mass_{6-AmHap-linker}$ were 682.27 and 725.31 g/mol respectively. Both conjugates had similar high number of ~32-36 haptens attached per TT molecule in several synthesis.

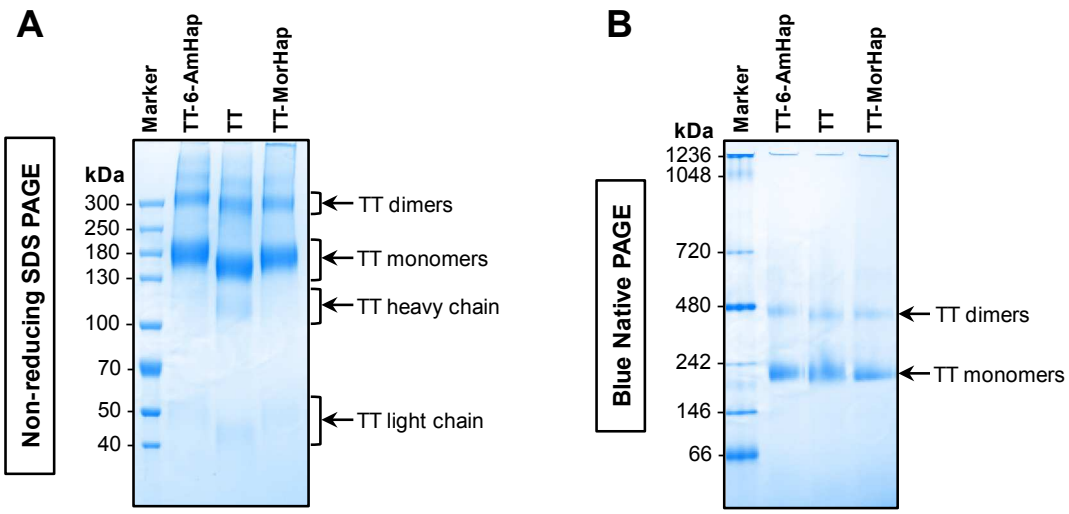

Figure S2. Analysis of heroin vaccine bioconjugates by protein gel electrophoresis. Non-reducing SDS PAGE (panel A) and Blue Native PAGE (panel B) gel analysis of unconjugated TT, TT-**1** (6-AmHap), and TT-**3** (MorHap) conjugates is shown. The molecular weight marker sizes (kDa) are indicated on the left, the various protein forms are indicated on the right and the samples loaded in each lane are indicated on top of the gels. All reagents were purchased from *Life Technologies* Corp., CA, USA and used as per the manufacturer's instructions.

For SDS PAGE, 5 µg of proteins were run under non-reducing conditions on NuPAGE Novex 4-12% Bis-Tris gels in MOPS running buffer (A). The reducing agent was omitted to avoid the thiol exchange of the thioether bond between the haptens and the maleimide end of the SM-$(PEG)_2$ linker. The gels were stained with the Imperial™ coomassie dye R-250 based protein stain (Cat # 24615). The Spectra™ multicolor high range protein ladder (Cat # 26625) was used as the marker. For unconjugated TT, the major band for the TT monomer (~150 kDa), the TT dimer (~300 kDa) and faint amounts of the TT heavy (~100 kDa) and light (~50 kDa) chains were observed. All these forms showed slight increase in sizes in the TT conjugates. Both TT-**1** and TT-**3** conjugates had similar sizes indicating similar hapten loading and none of them had high molecular weight protein aggregates.

For native PAGE, 5 µg of the same samples were mixed with the NativePAGE™ sample buffer and run on NativePAGE 4-16% Bis-Tris gels in NativePAGE running buffer that contains Coomassie G-250 as a charge-shift molecule in the cathode buffer instead of SDS (B). The NativeMark™ unstained protein standard (Cat # LC0725) was used as the marker. The dimeric and monomeric forms were observed for TT and the TT conjugates. Blue Native PAGE analysis confirmed the absence of protein aggregates in any sample, which is required for an ideal vaccine candidate.

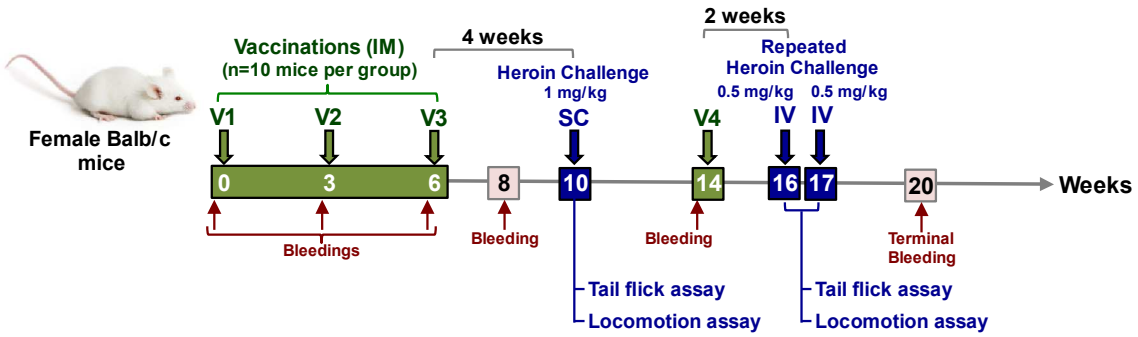

Fig S3. Study design for testing of TT-1 and TT-3 heroin vaccines in mice. Vaccine administration (V1-V3), bleeding, subcutaneous (SC) and intravenous (IV) heroin challenges are indicated by arrows. Groups of 10 mice each were intramuscularly (IM) immunized at weeks 0, 3, and 6 with either TT-**1** + ALF or TT-**3** + ALF. All mice were bled prior to each vaccination and 2 weeks (week 8) before heroin challenge. At week 10, mice were challenged with SC heroin (1 mg/kg). The mice were immunized at week 14 and then re-challenged with IV heroin at weeks 16 and 17. The vaccine efficacy upon heroin challenge was monitored by the tail flick and locomotion assays. At week 20, the mice were euthanized and the blood was collected by cardiac puncture.

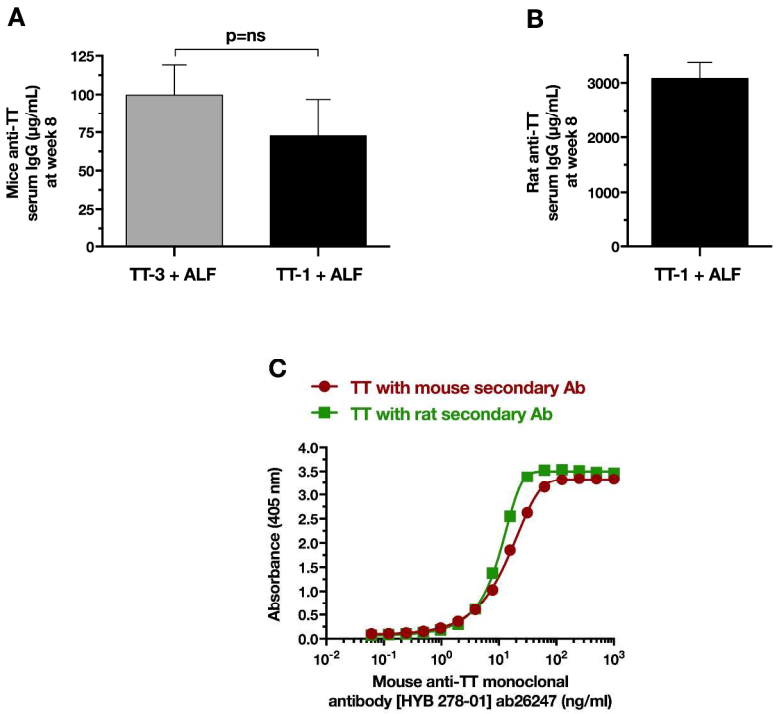

Figure S4. Anti-TT serum IgG levels at week 8 in mice and rats. Both TT-**1** and TT-**3** generated similar anti-TT levels in mice (A, p=ns). The anti-TT levels in TT-**1** vaccinated rats (B) were ~40-fold higher than in mice probably due to 10-fold higher doses of antigen and MPLA used and were maintained at similar levels at week 14 (data not shown). Both mouse and rat secondary antibodies bound well to the mouse anti-tetanus toxoid (TT) monoclonal antibody [HYB-278-01] (AbCam, Cat. No. ab26247) (C) that was used as standard curve for quantification of serum TT carrier protein specific IgG levels in mice (A) and rats (B) as described previously.[2]

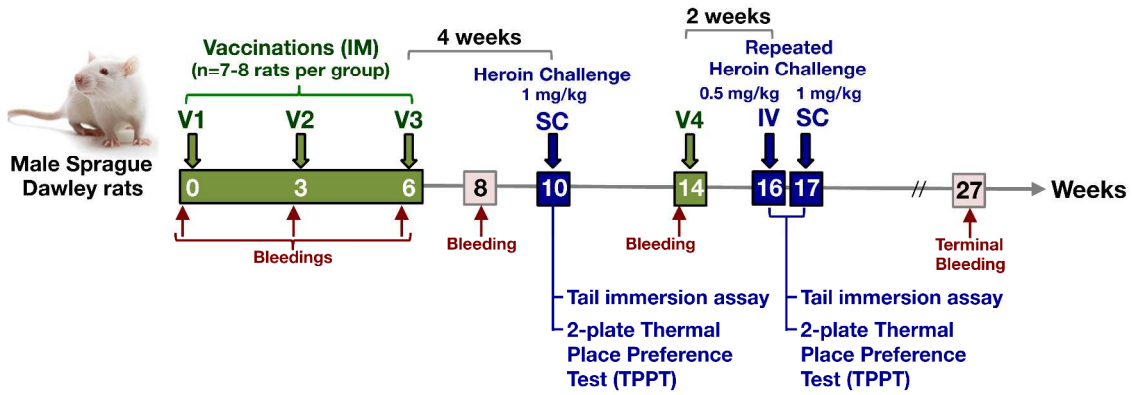

Figure S5. Study design for testing of TT-1 heroin vaccines in rats. Vaccine administration (V1-V3), bleeding, subcutaneous (SC) and intravenous (IV) heroin challenges are indicated by arrows. Eight rats were intramuscularly (IM) immunized at weeks 0, 3, and 6 with TT-**1** + ALF. All rats were bled prior to each vaccination and 2 weeks (week 8) before heroin challenge. At week 10, rats were challenged with SC heroin (1 mg/kg). The rats were immunized at week 14 and then re-challenged with IV and SC heroin at weeks 16 and 17, respectively. The vaccine efficacy upon heroin challenge was monitored by the tail immersion assay and thermal place preference test (TPPT). At week 27, the rats were euthanized and the blood was collected by cardiac puncture.

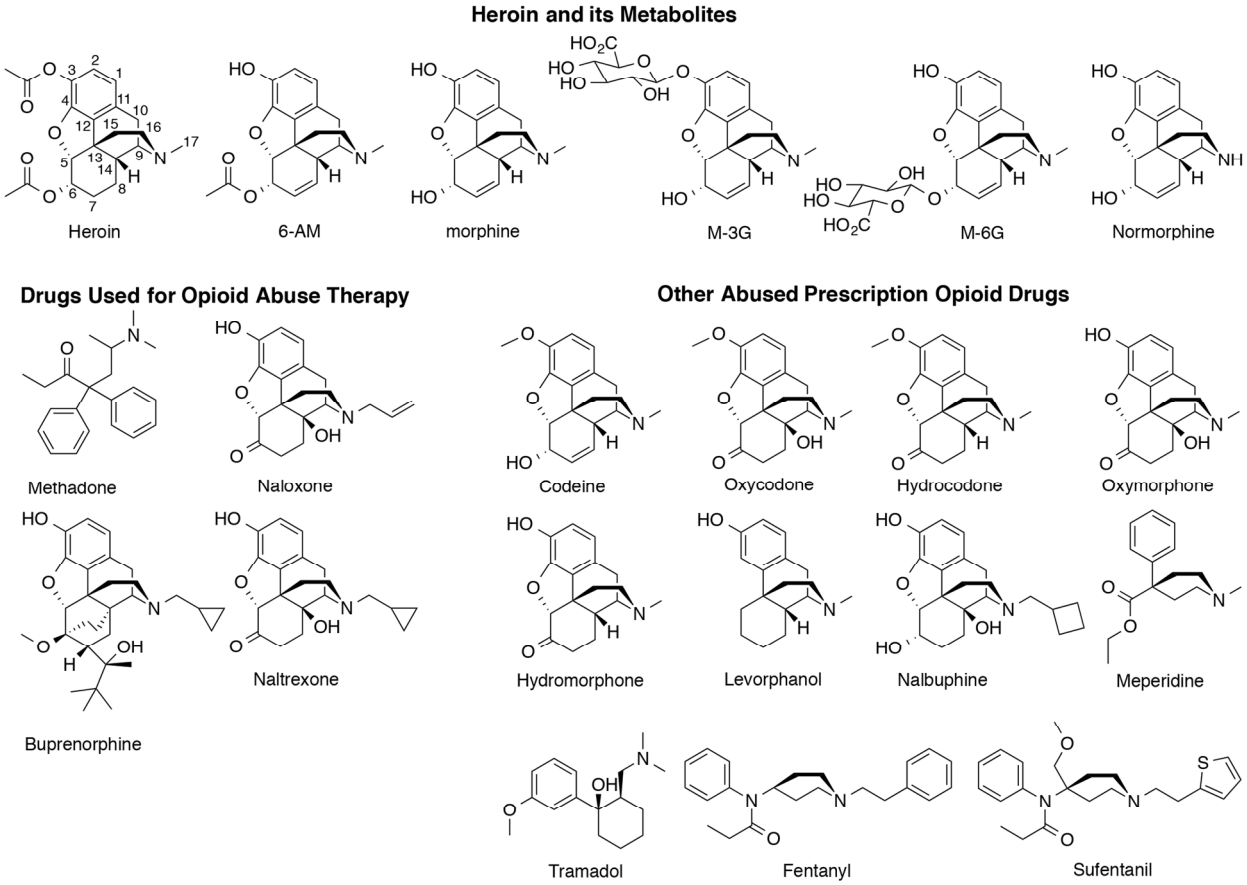

Figure S6. Structures of the drugs, which were used in the competition ELISA.

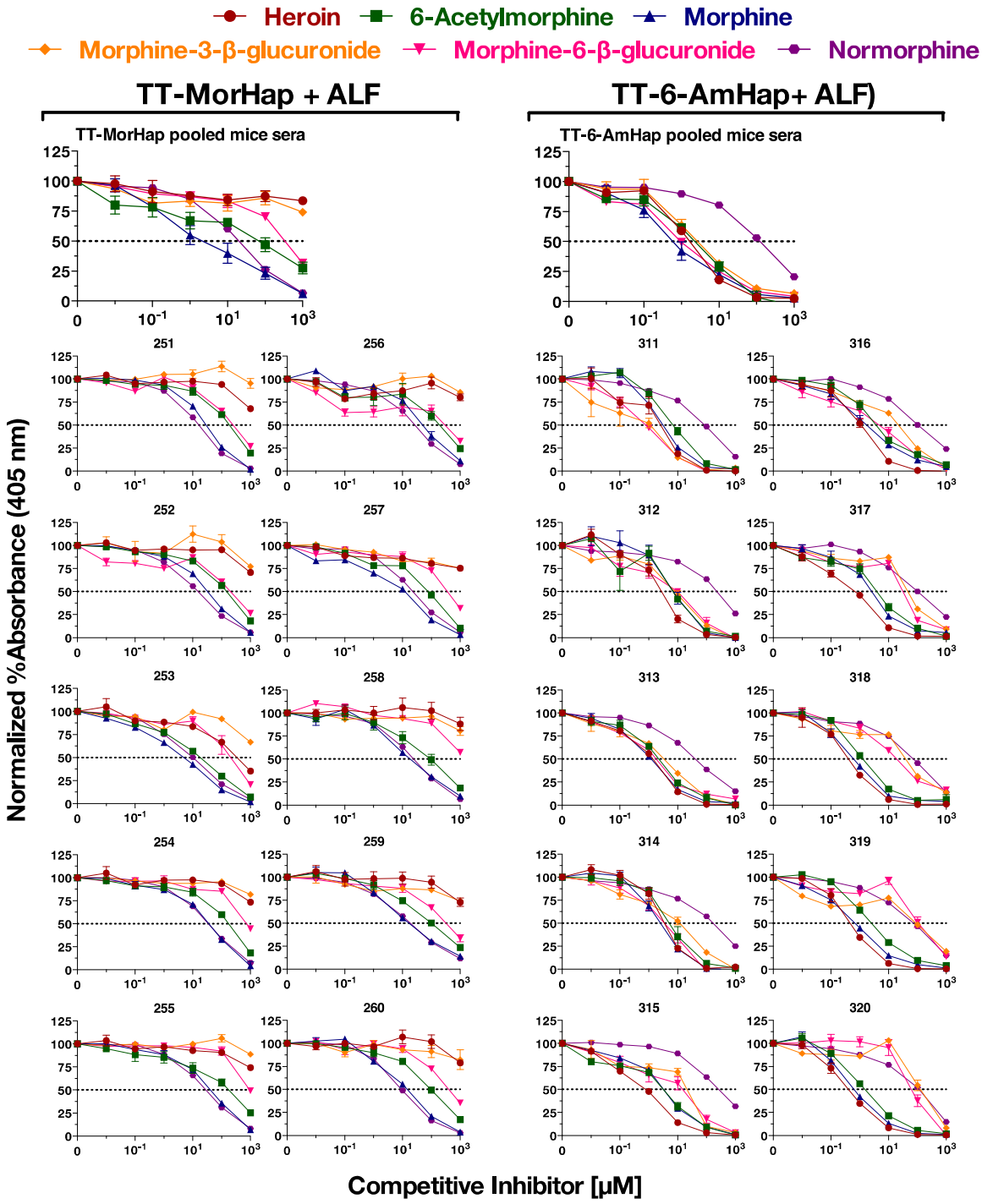

Figure S7. Competitive inhibition in ELISA for the binding of mouse 1 and 3 induced antibodies by heroin and its metabolites. Normalized competition ELISA curves showing Mean ± SEM of triplicate determinations from pooled and individual mice sera from week 8 are shown. IC_{50} values were calculated and are shown in supplemental Table S1 on page S32. TT-**1** generated antibodies with significantly higher affinities for heroin and its active metabolites than TT-**3**.

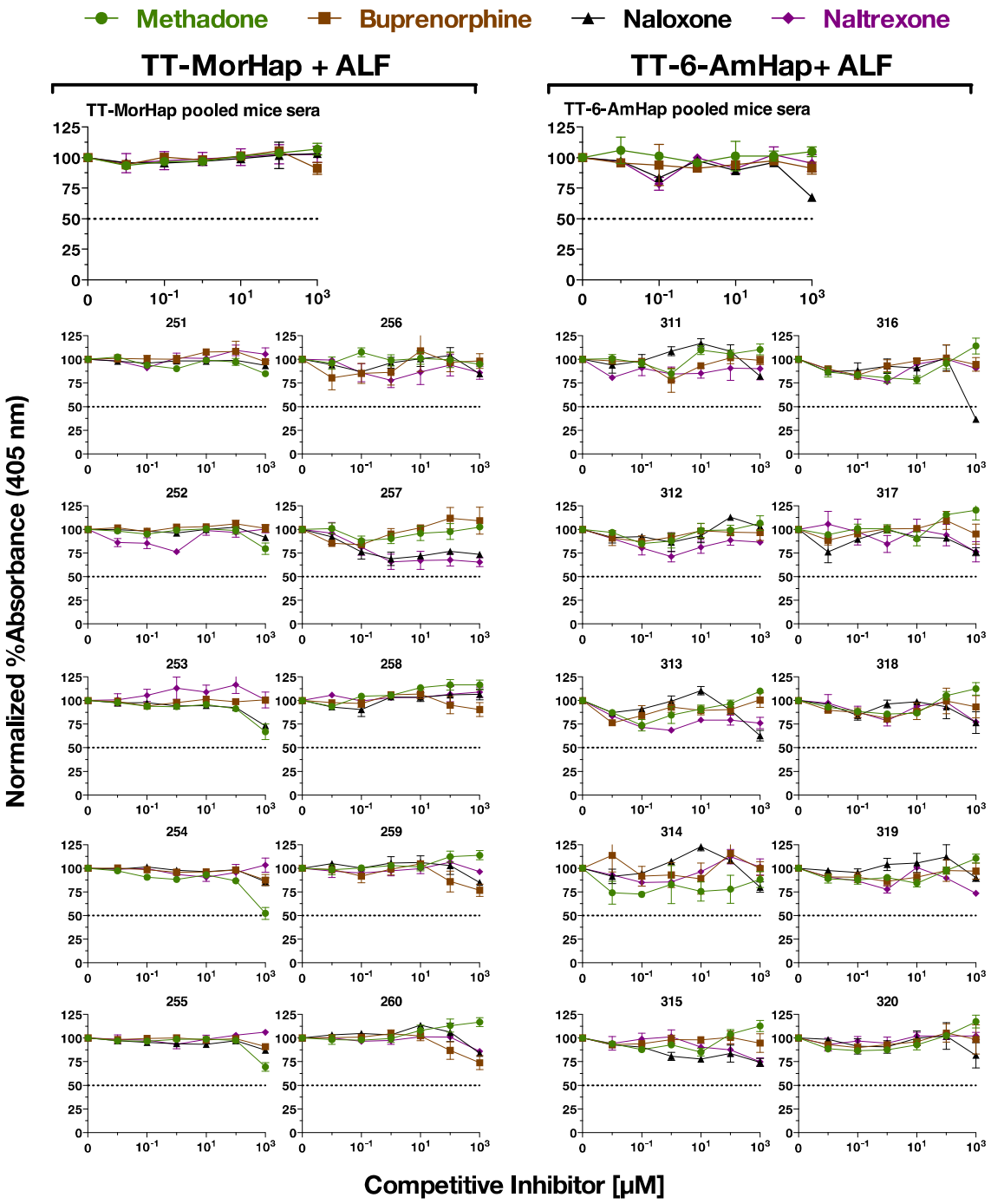

Figure S8. Competitive inhibition in ELISA for the binding of mouse 1 and 3 induced antibodies by drugs used for opioid abuse therapy. Normalized competition ELISA curves showing Mean ± SEM of triplicate determinations from pooled and individual mice sera from week 8 are shown. IC_{50} for all drugs was >1000 for all samples indicating no binding of the hapten antibodies to these drugs. Hence, immunization with these heroin vaccines would not interfere with the pharmacotherapy of patients undergoing treatment for heroin addiction. This is an essential requirement for any potential heroin vaccine.

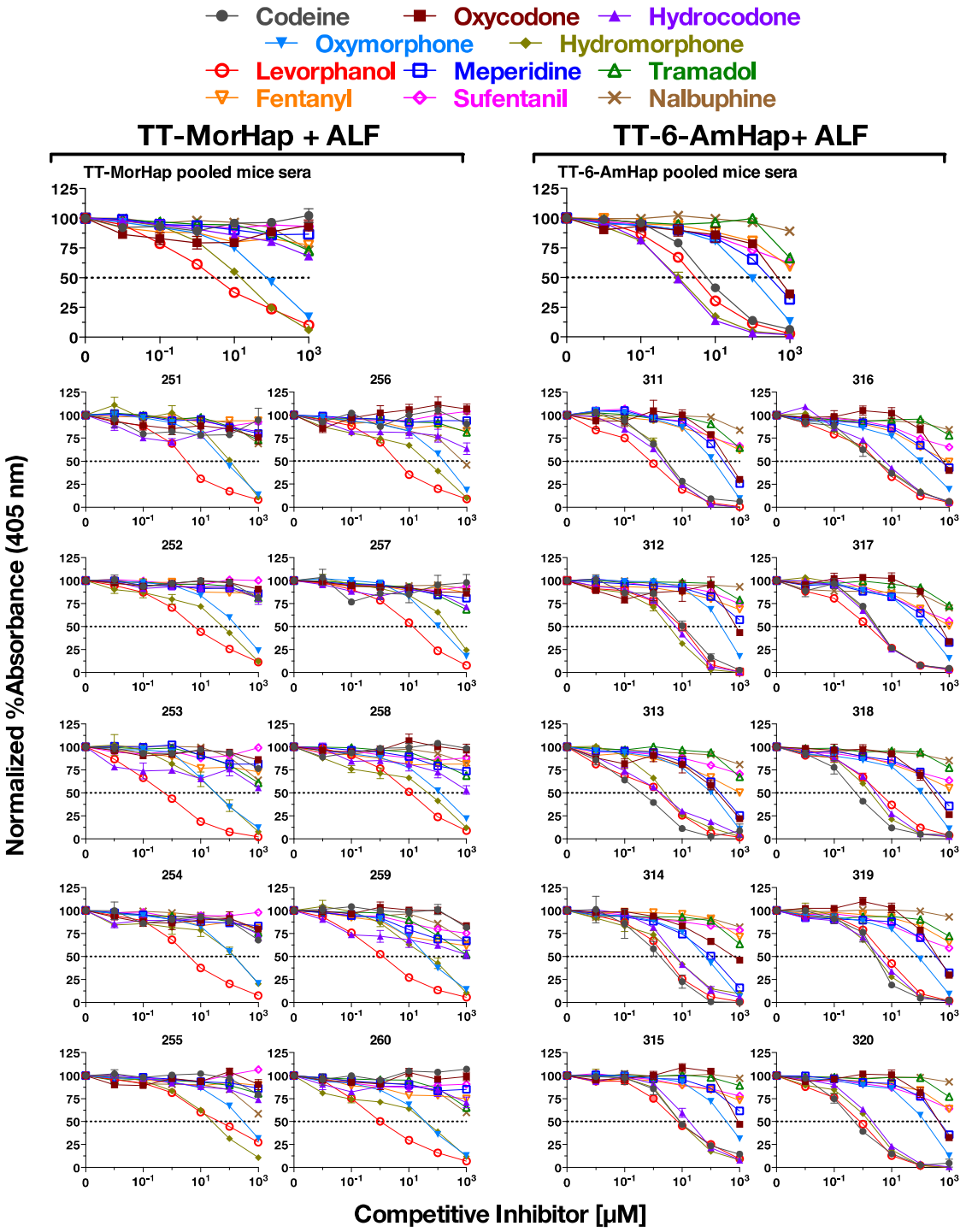

Figure S9. Competitive inhibition in ELISA for the binding of mouse 1 and 3 induced antibodies by other abused prescription opioid drugs. Normalized competition ELISA curves showing Mean ± SEM of triplicate determinations from pooled and individual mice sera from week 8 are shown. IC_{50} values were calculated and are shown in supplemental Table S1 on page S32. Unlike **3**, **1** induced antibodies cross-reacted with several other abused opioids, indicating its potential as a broad opioid vaccine.

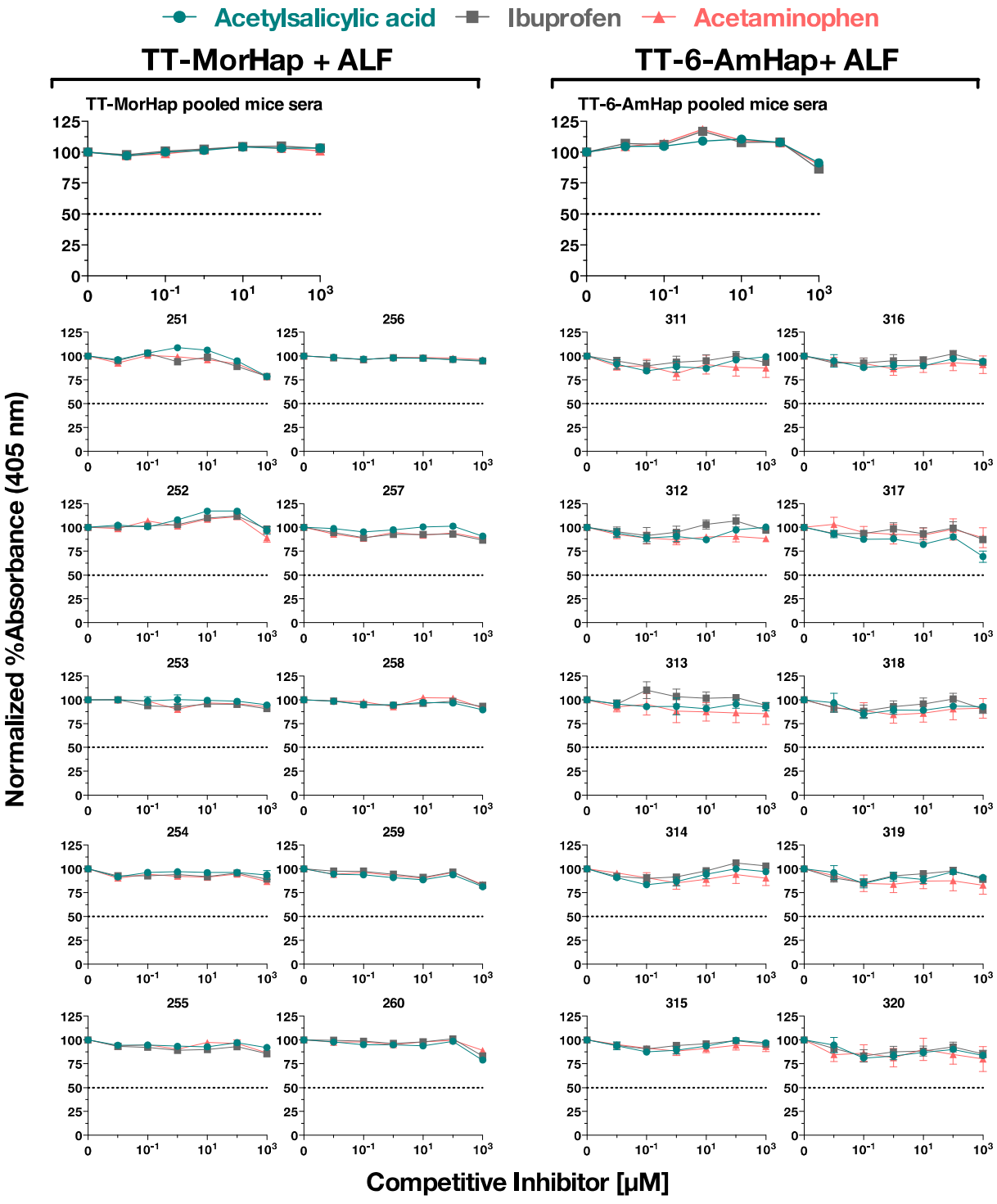

Figure S10. Competitive inhibition in ELISA for the binding of mouse 1 and 3 induced antibodies by non-narcotic analgesics. Normalized competition ELISA curves showing Mean ± SEM of triplicate determinations from pooled and individual mice sera from week 8 are shown. IC_{50} for all drugs was >1000 for all samples indicating no binding of the hapten antibodies to these drugs. Hence, these drugs could be used in the immunized individuals for routine pain management.

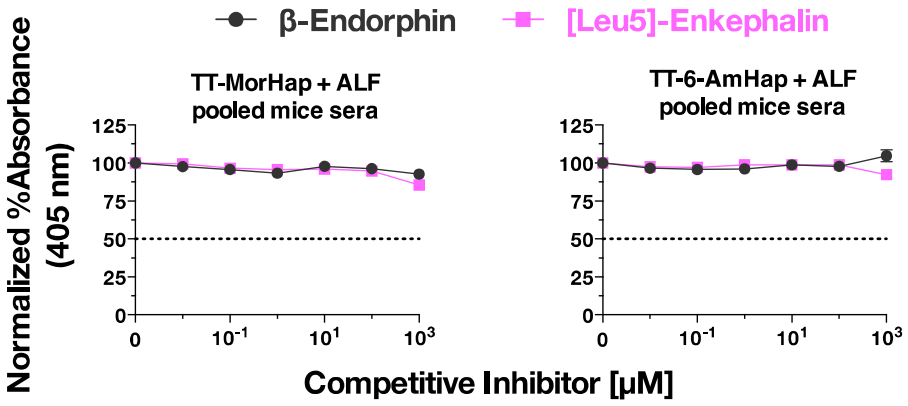

Figure S11. Competitive inhibition in ELISA for the binding of 1 and 3 induced antibodies by endogenous opioid peptides. Normalized competition ELISA curves showing Mean ± SEM of triplicate determinations from pooled mice sera from week 8 are shown. IC_{50} for both peptides was >1000 for both groups indicating no binding of the hapten antibodies to these peptides. Hence, the vaccine would not block the effects of these endogenous opioid neuropeptides, which is an essential requirement for any potential heroin vaccine.

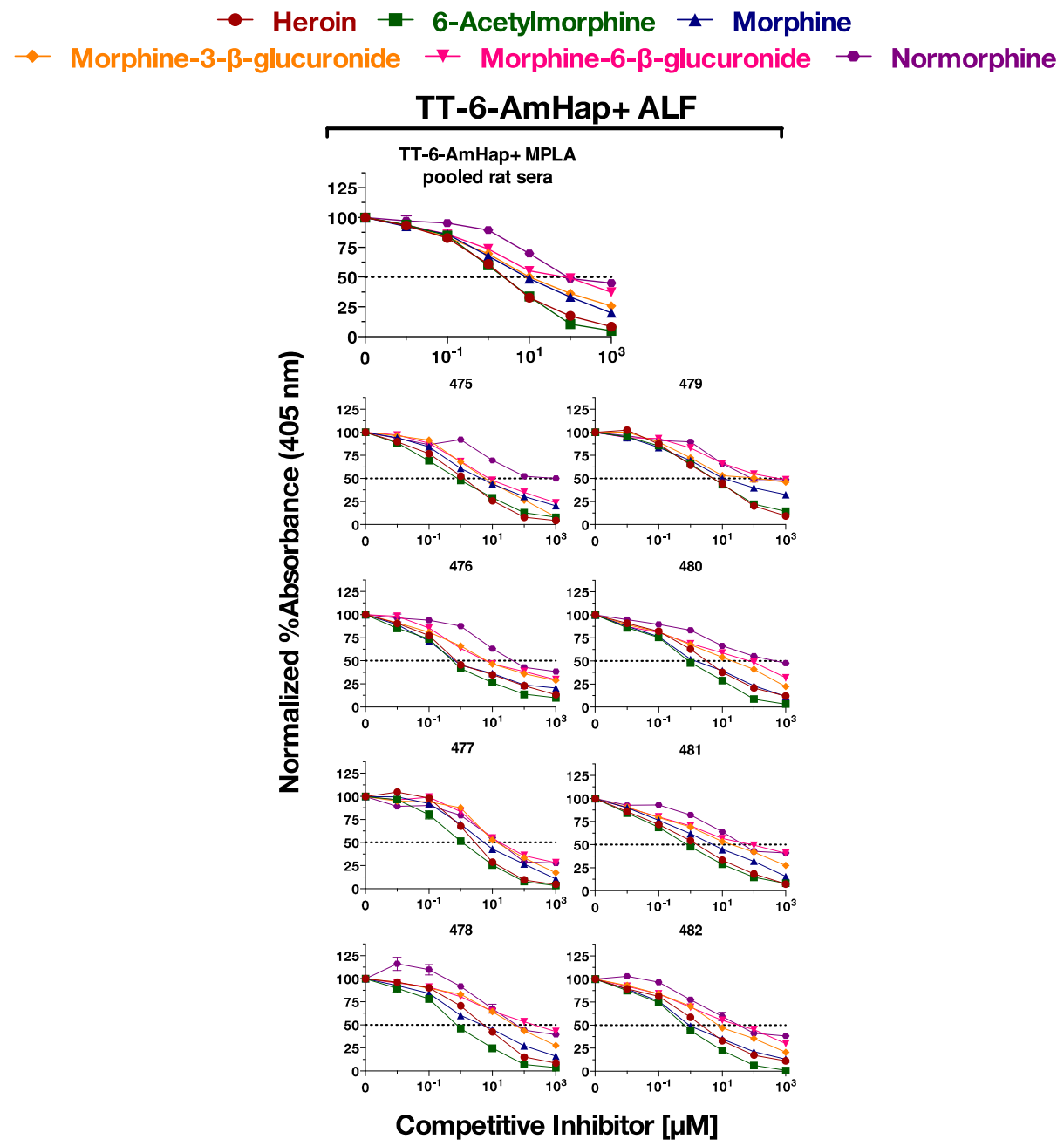

Figure S12. Competitive inhibition in ELISA for the binding of rat 1 induced antibodies by heroin and its metabolites. Normalized competition ELISA curves showing Mean ± SEM of triplicate determinations from pooled and individual rat sera from week 8 are shown. IC_{50} values were calculated and are shown in supplemental Table S2 on page S33. TT-**1** with ALF as adjuvant generated antibodies with high affinities for heroin and its active metabolites in rats as well.

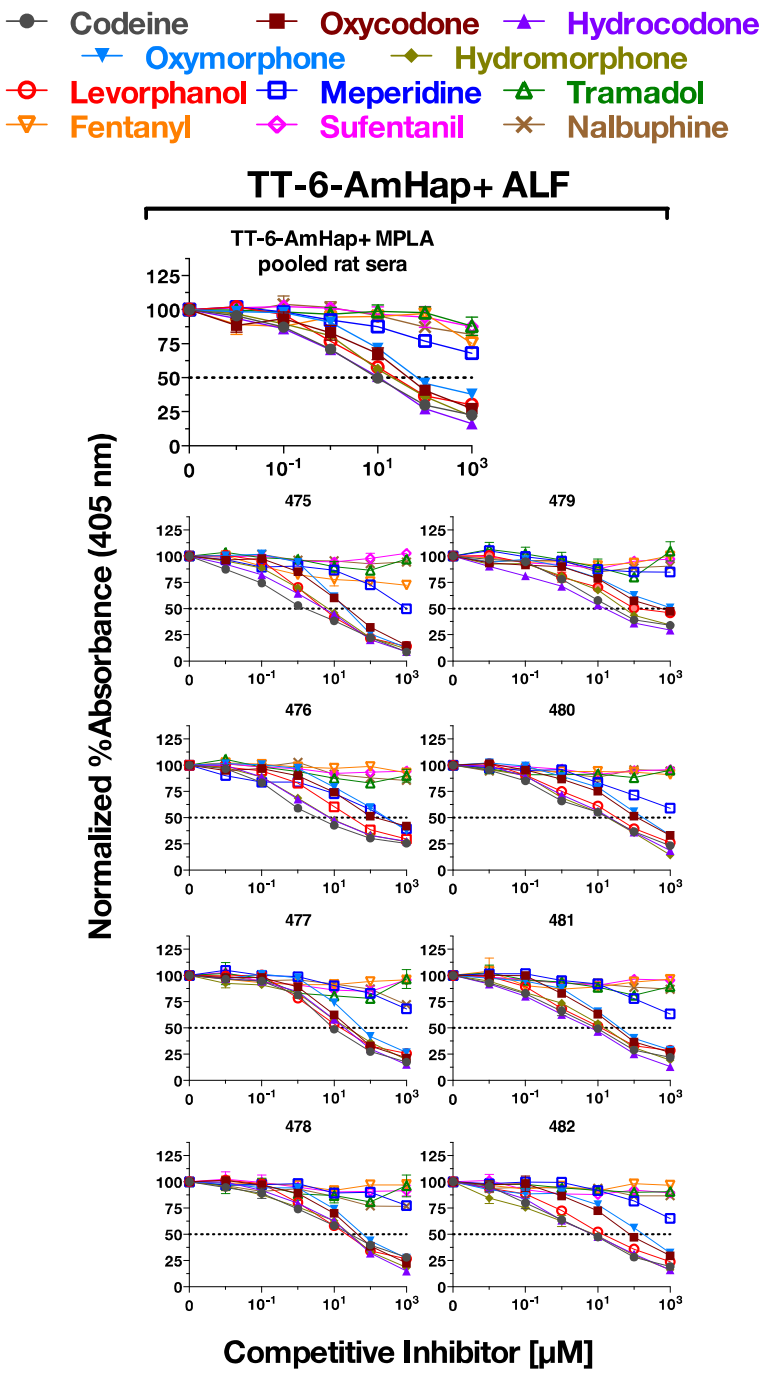

Figure S13. Competitive inhibition in ELISA for the binding of rat 1 induced antibodies by other abused prescription opioid drugs. Normalized competition ELISA curves showing Mean ± SEM of triplicate determinations from pooled and individual rat sera from week 8 are shown. IC_{50} values were calculated and are shown in supplemental Table S2 on page S33. As seen for mice, rat **1** induced antibodies also cross-reacted with several other abused opioids, reconfirming their potential as a broad opioid vaccine.

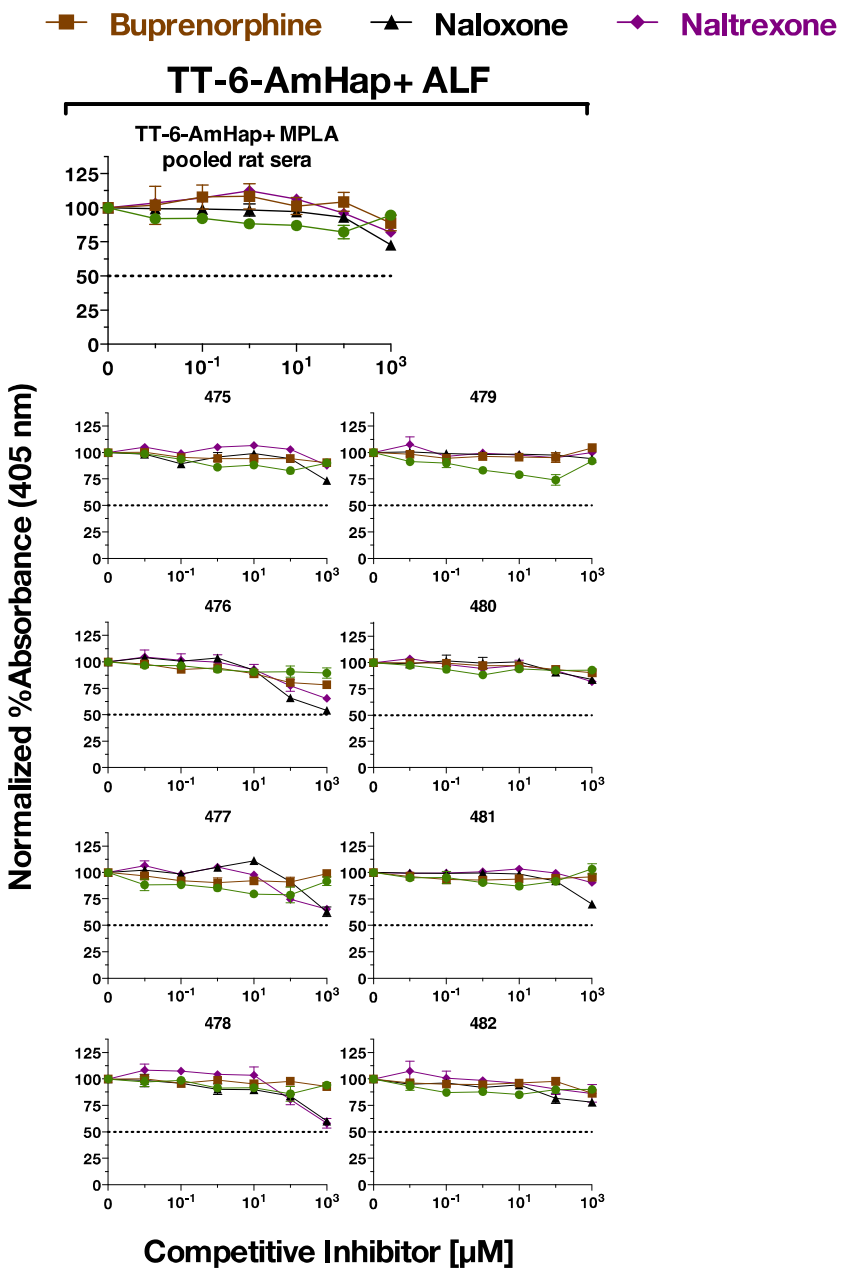

Figure S14. Competitive inhibition in ELISA for the binding of rat 1 induced antibodies by drugs used for opioid abuse therapy. Normalized competition ELISA curves showing Mean ± SEM of triplicate determinations from pooled and individual rat sera from week 8 are shown. As seen for mice, the IC_{50} for all drugs was >1000 for all rat samples as well. This reconfirmed that the **1** induced antibodies would not bind and interfere with these drugs used for drug addiction therapy.

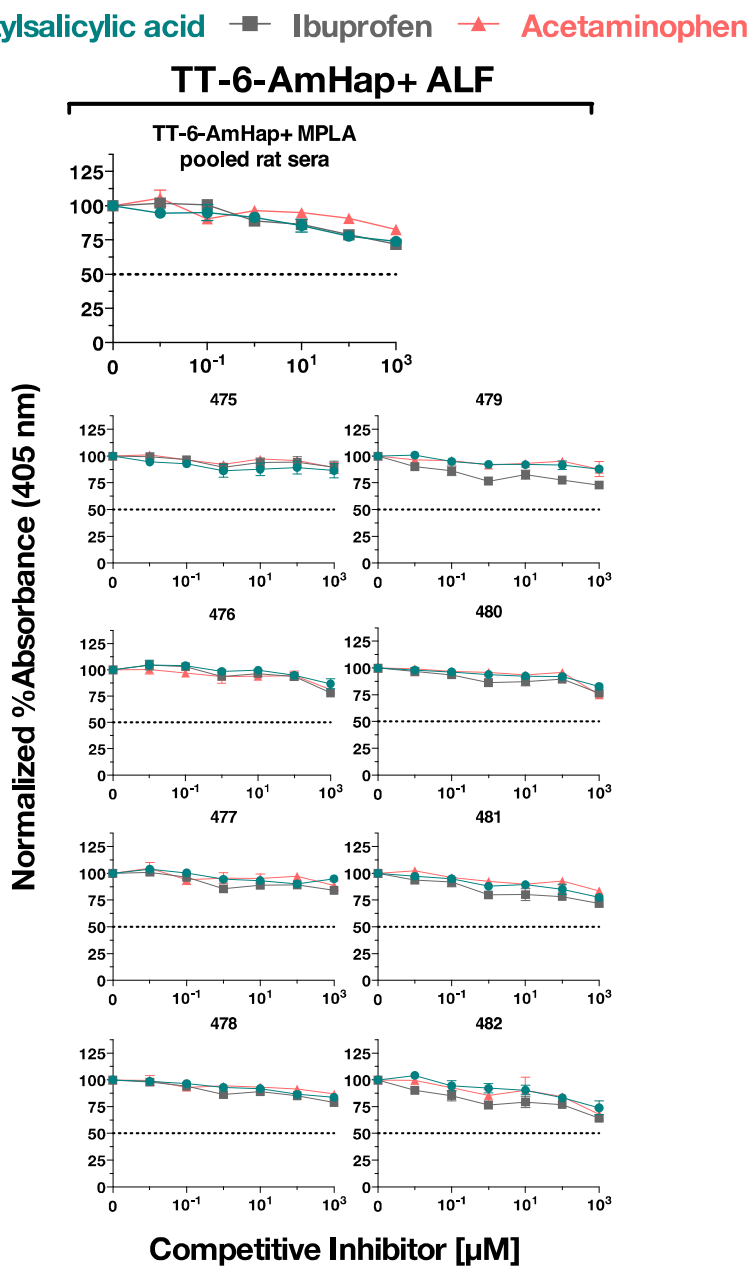

Figure S15. Competitive inhibition in ELISA for the binding of rat 1 induced antibodies by non-narcotic analgesics. Normalized competition ELISA curves showing Mean ± SEM of triplicate determinations from pooled and individual rat sera from week 8 are shown. As seen for mice, the IC_{50} for all these drugs was >1000 for all rat samples as well. This reconfirmed that the **1** induced antibodies would not bind these drugs and they could be effectively used in TT-**1** immunized individuals for routine pain management.

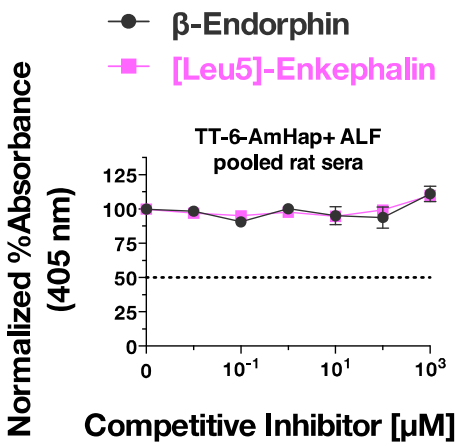

Figure S16. Competitive inhibition in ELISA for the binding of rat 1 induced antibodies by endogenous opioid peptides. Normalized competition ELISA curves showing Mean ± SEM of triplicate determinations from pooled rat sera from week 8 are shown. As seen for mice, the IC_{50} for both peptides was >1000 for rat sera as well indicating no binding of the **1** induced antibodies to these peptides. This reconfirmed that the vaccine would not block the effects of these endogenous opioid neuropeptides in immunized individual

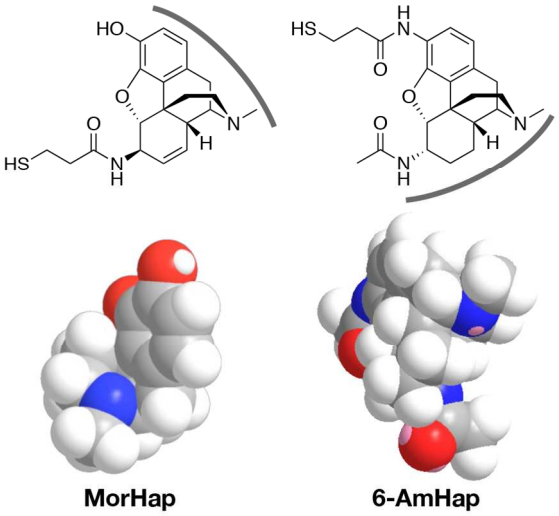

Figure S17. Facial recognition of 1 (6-AmHap) and 3 (MorHap). Because of conjugation to TT, the freedom of motion of the hapten is restricted. Consequently, the structure of the hapten structure bifurcates into two immunologically defined "faces". The "front face" constitutes the functional groups that are exposed to the immune system and the "back face" is the sterically blocked moieties near the conjugation site.[4] The gray arcs indicate the hypothetical front face of **1** and **3** (Top). The space-filling models (ChemBio3D Ultra) show the minimized energy configuration of the haptens (Bottom).

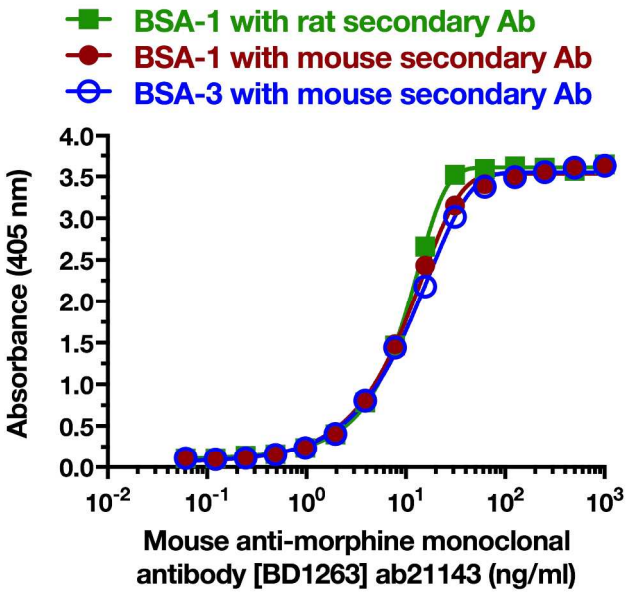

Figure S18. Comparison of anti-morphine ELISA standard curves using different haptens and secondary antibodies. ELISA Standard curves were run and compared using BSA-**1** or BSA-**3** conjugates as the coating antigen with mouse anti-morphine monoclonal antibody (mAb) [BDI263] (Abcam, Cambridge, MA; Cat. No. ab21143) as primary antibody followed by peroxidase linked mouse or rat secondary antibodies (sAb) using ELISA methods as described below. The nonlinear regression curve fit of **3** with mouse sAb and of **1** with mouse or rat sAb were similar ($p>0.05$) in the linear range (OD 0.2 to 3.2). This allowed for the quantification and mutual comparison of the hapten-specific serum IgG levels for both haptens in mice and rats using the same anti-morphine mAb as shown in Figure 4 and Figure 7.

Binding ELISA was performed as described before.[1, 2] The BSA-**1** or BSA-**3** conjugates for ELISA were prepared using a low BSA to $SM(PEG)_2$ linker ratio of 1:10 for conjugation which gave low hapten density of ~4 to 5 haptens attached per BSA molecule as measured by MALDI-TOF MS. Low hapten density BSA-hapten conjugates were used for ELISA as they gave lower steric hindrance and optimal antibody binding as reported before [1]. The BSA-**1** or BSA-**3** conjugate or TT (0.1 µg/0.1 ml/well in PBS) were added to the Nunc MaxiSorp® flat-bottom ELISA plates and incubated at 4 ºC overnight. The plates were blocked with 1% BSA in TBS (20 mM Tris, 154 mM sodium chloride) for mouse samples or with 0.5% milk, 0.1% Tween-20 in PBS for rat samples at pH 7.4 for 2 h. The blocker was removed and sera, serially diluted in the appropriate blocker in triplicates, were added to the plates. Following incubation for 1 h at room temperature, the plates were washed with TBS, 0.1% Tween-20. Peroxidase linked sheep anti-mouse IgG (The Binding Site, San Diego, CA) or goat anti-rat IgG (Bethyl Laboratories, Inc., Montgomery, TX) diluted in blocker was added and the plates were incubated for 1 h at room temperature. The plates were washed and ABTS substrate (KPL, Inc., Gaithersburg, MD) was added. After 1 h incubation at room temperature, color development was stopped by adding 100 µl/well of 1% SDS and the absorbance was read at 405 nm. Serum IgG concentrations were quantified for both mouse and rat samples using corresponding standard curves of murine anti-morphine mAb BDI263 for both haptens as shown above and mouse anti-TT mAb HYB-278-01 (AbCam) for TT (Figure S4).

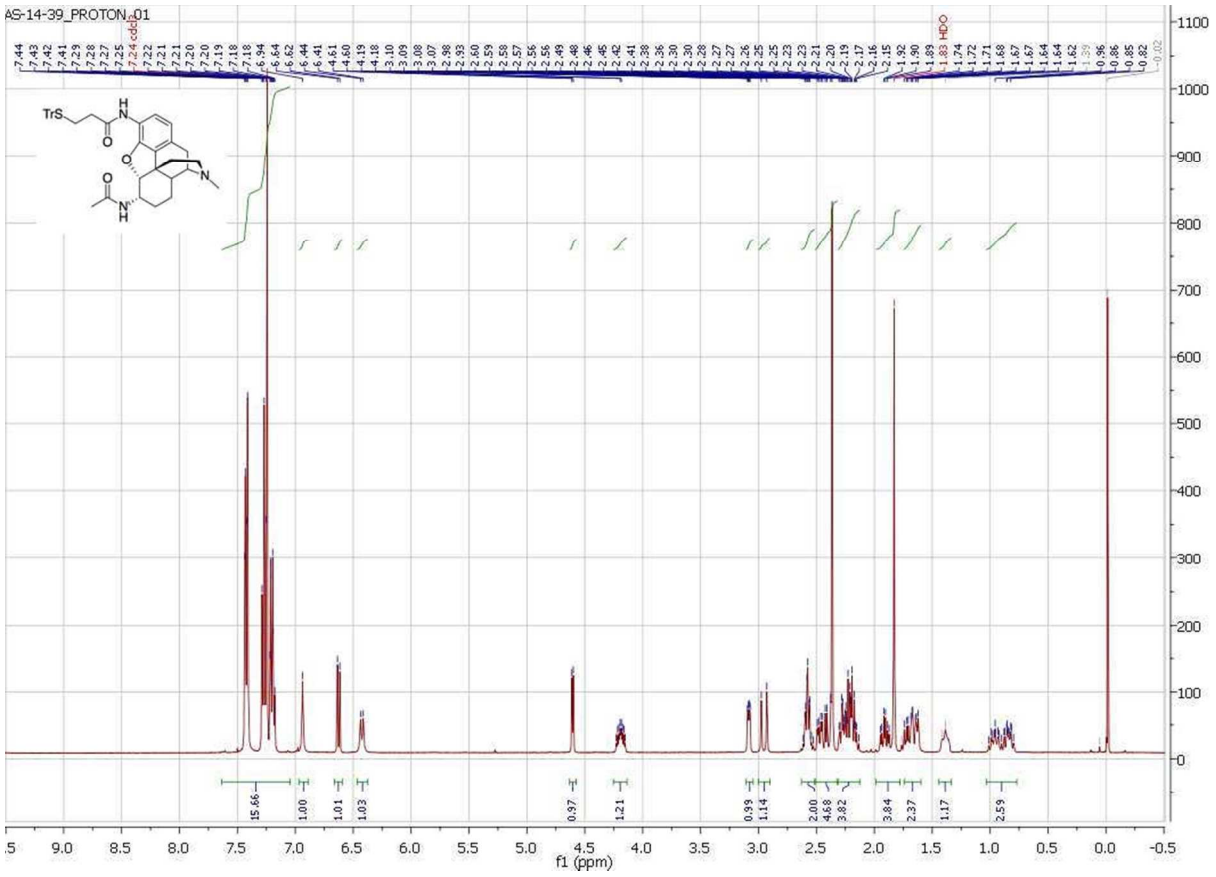

Figure S19. ^{1}H NMR of **1**

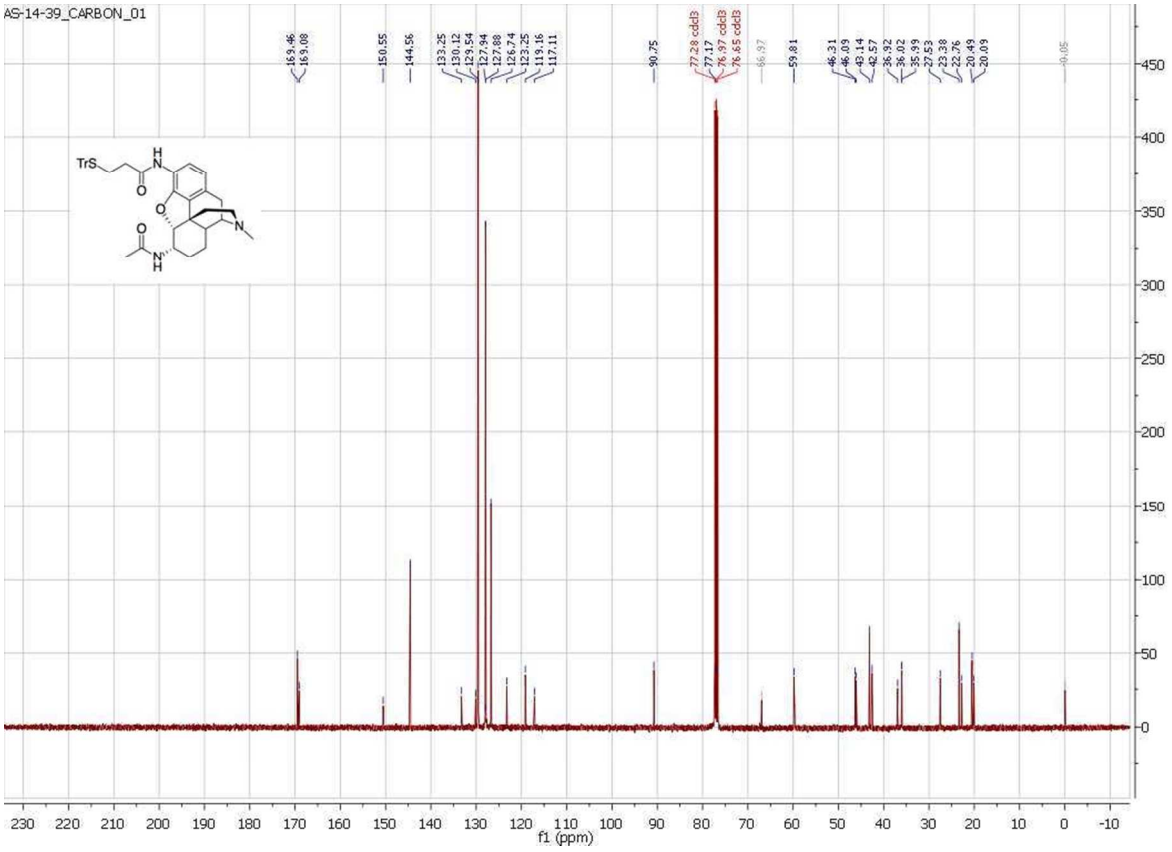

Figure S20. ^{13}C NMR of **1**

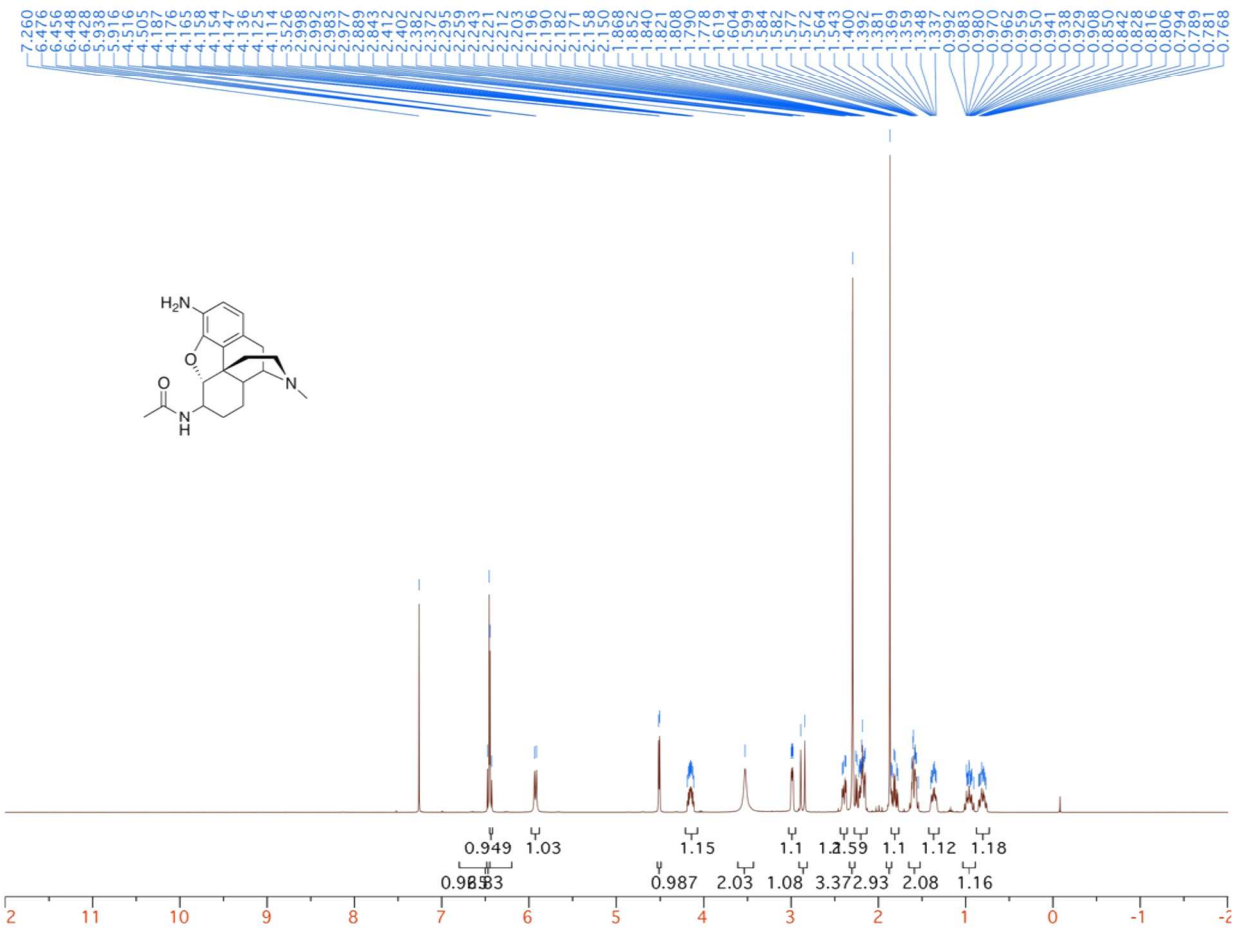

Figure S21. ^{1}H NMR of 12

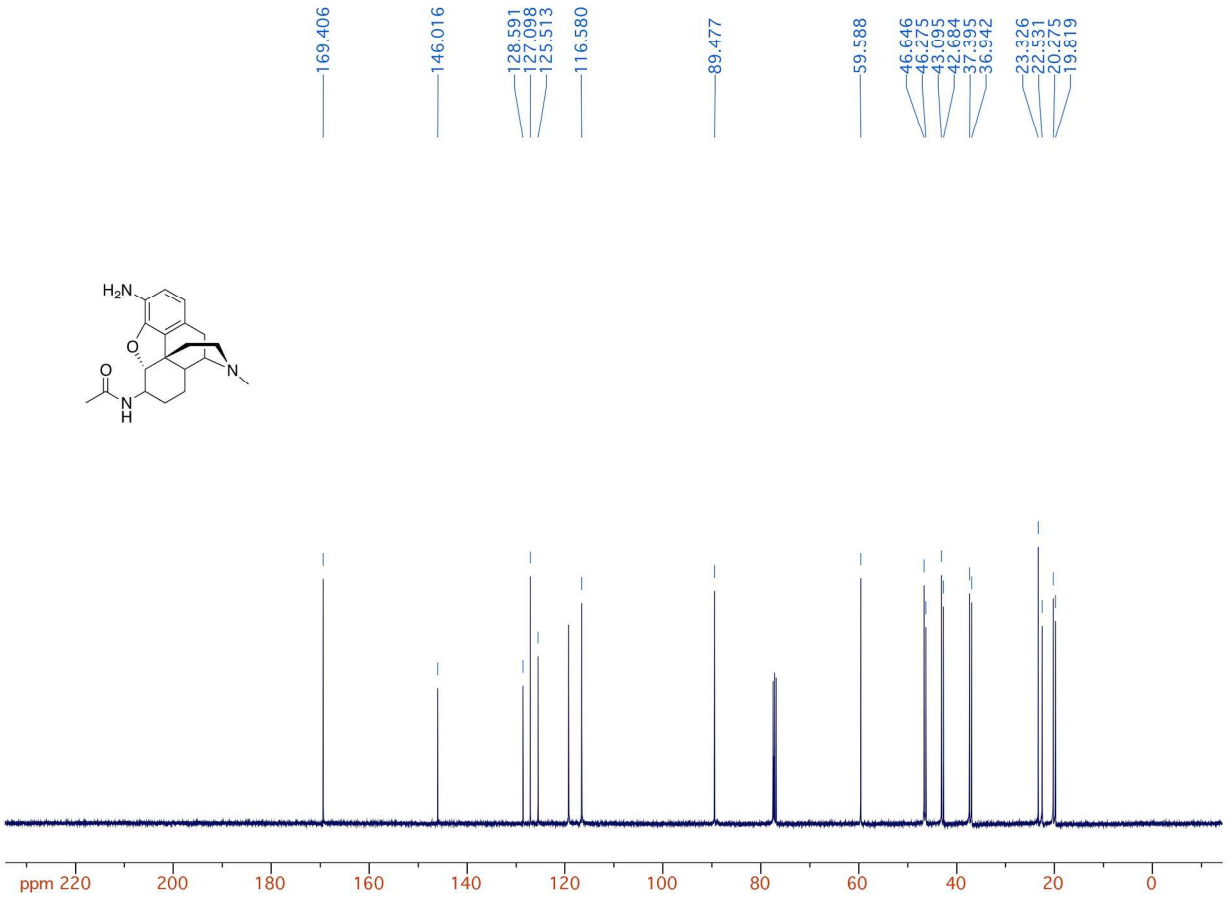

Figure S22. ^{13}C NMR of **12**

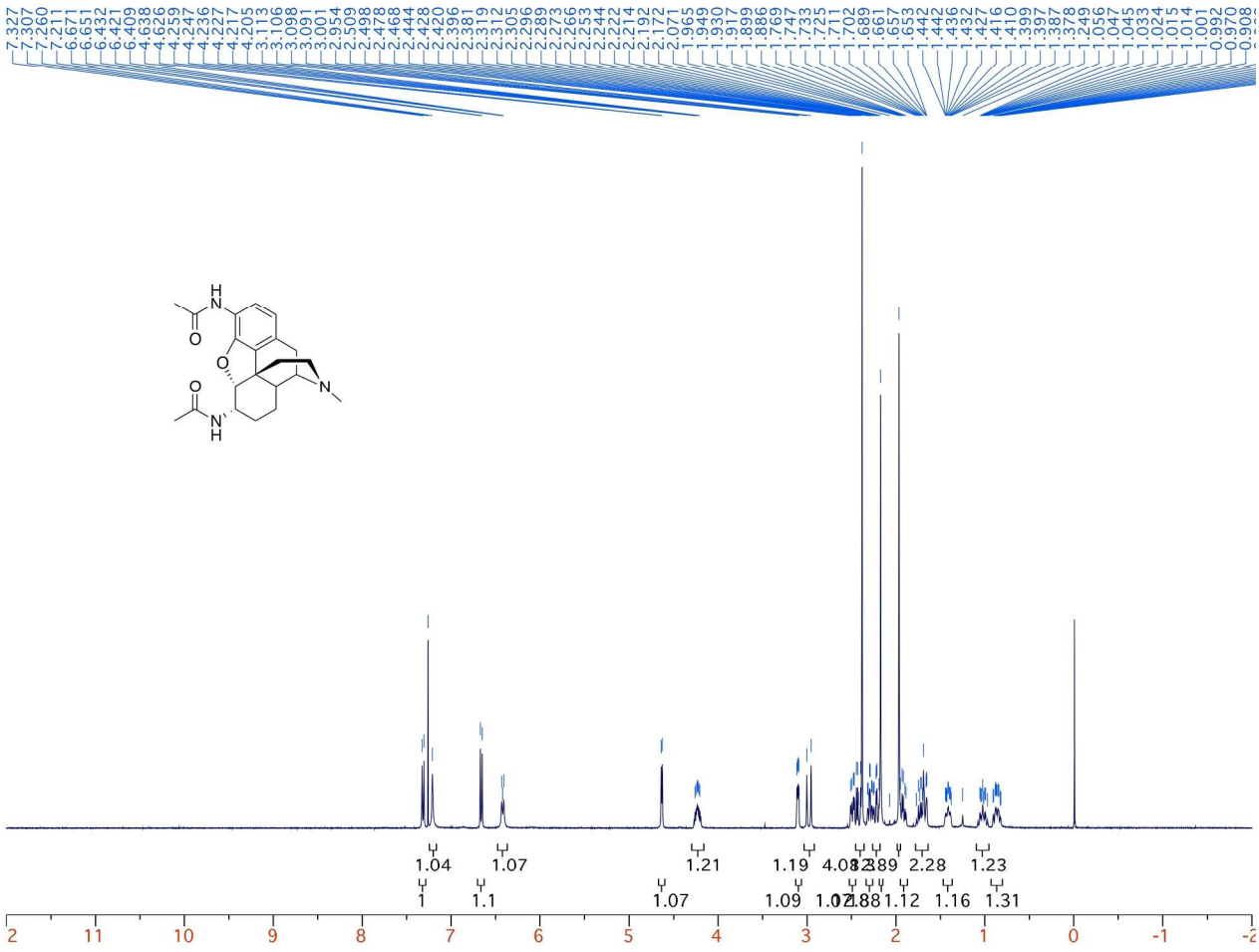

Figure S23. ^{1}H NMR of **13**

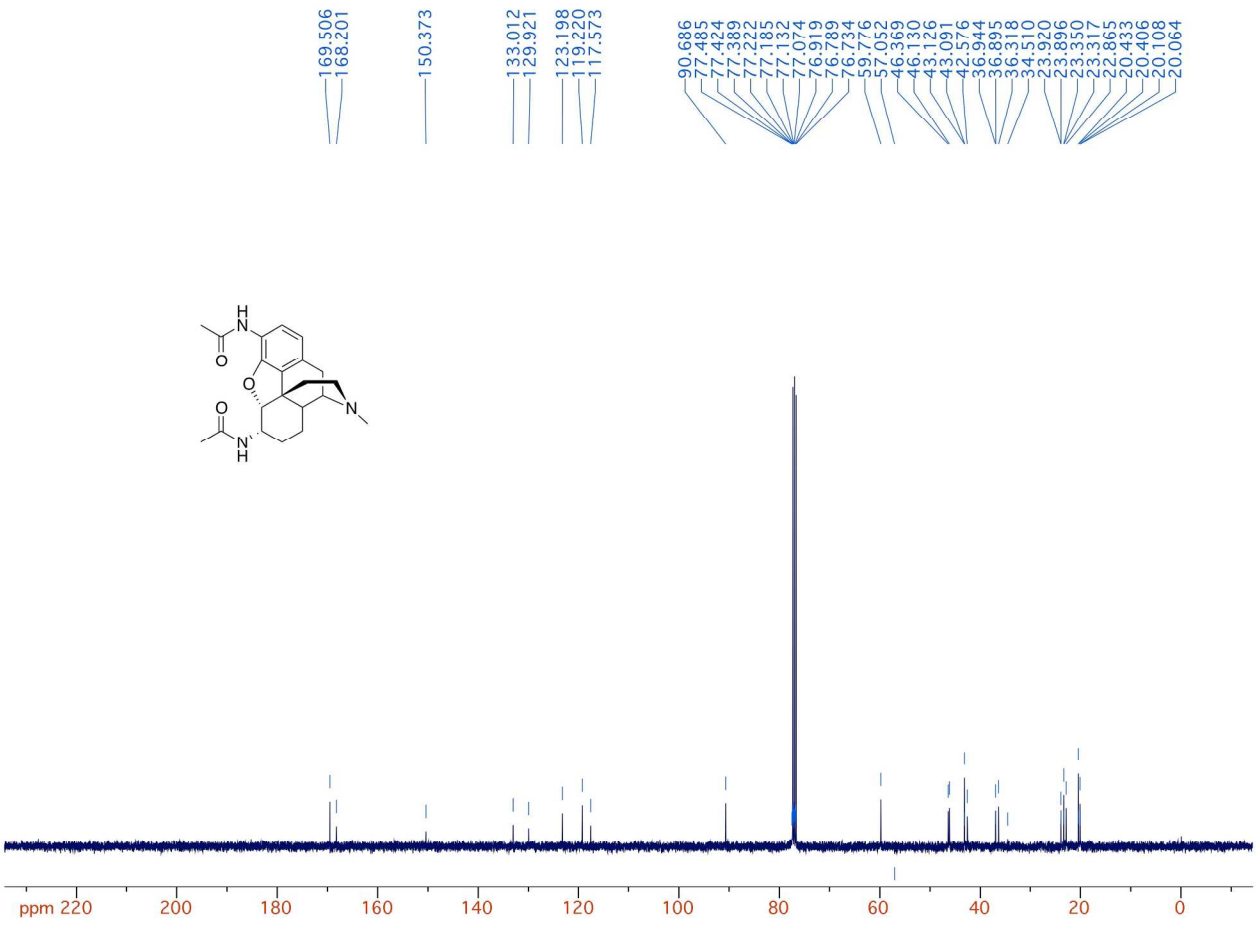

Figure S24. ^{13}C NMR of **13**

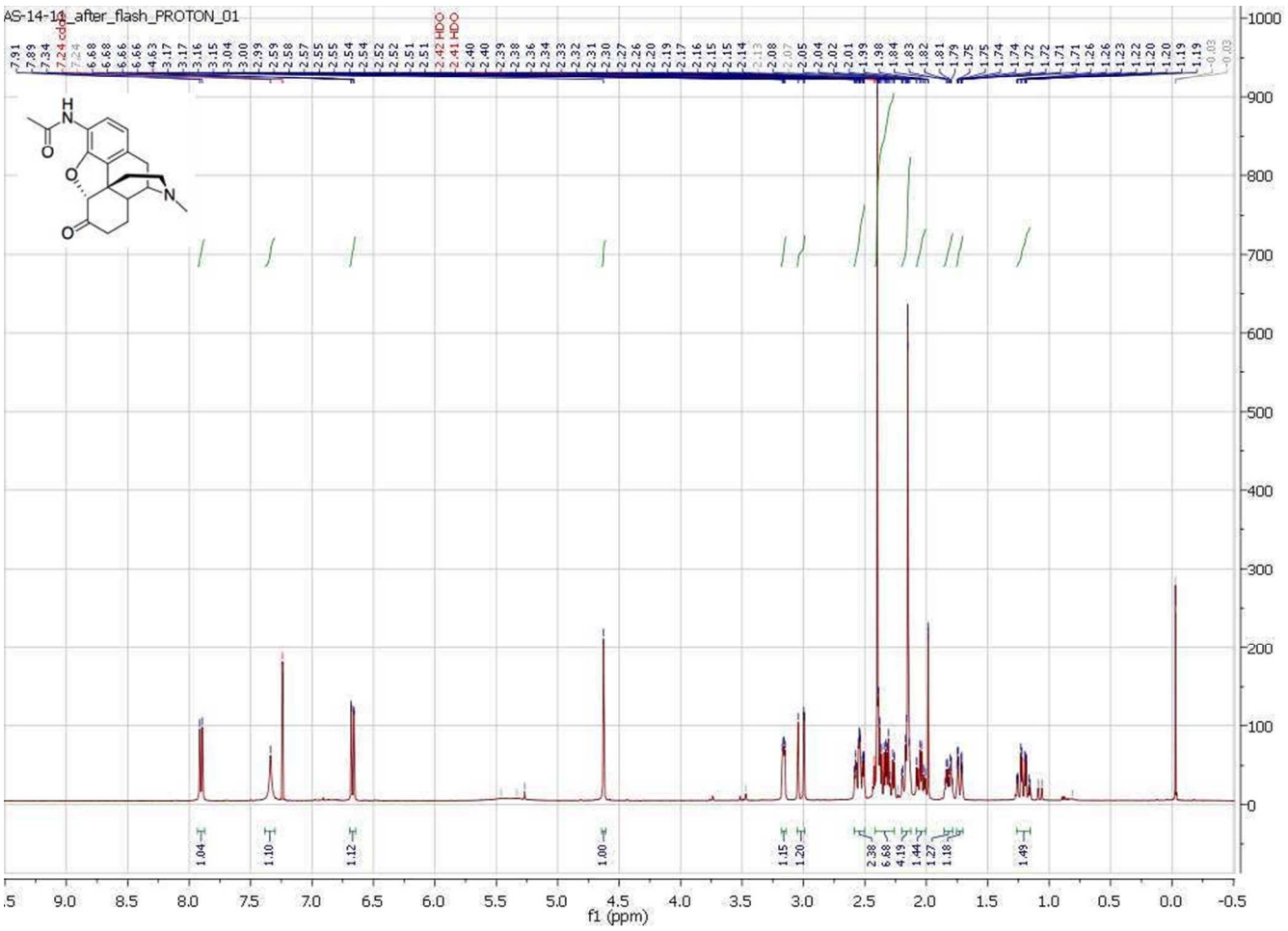

Figure S25. ^{1}H NMR of **15**

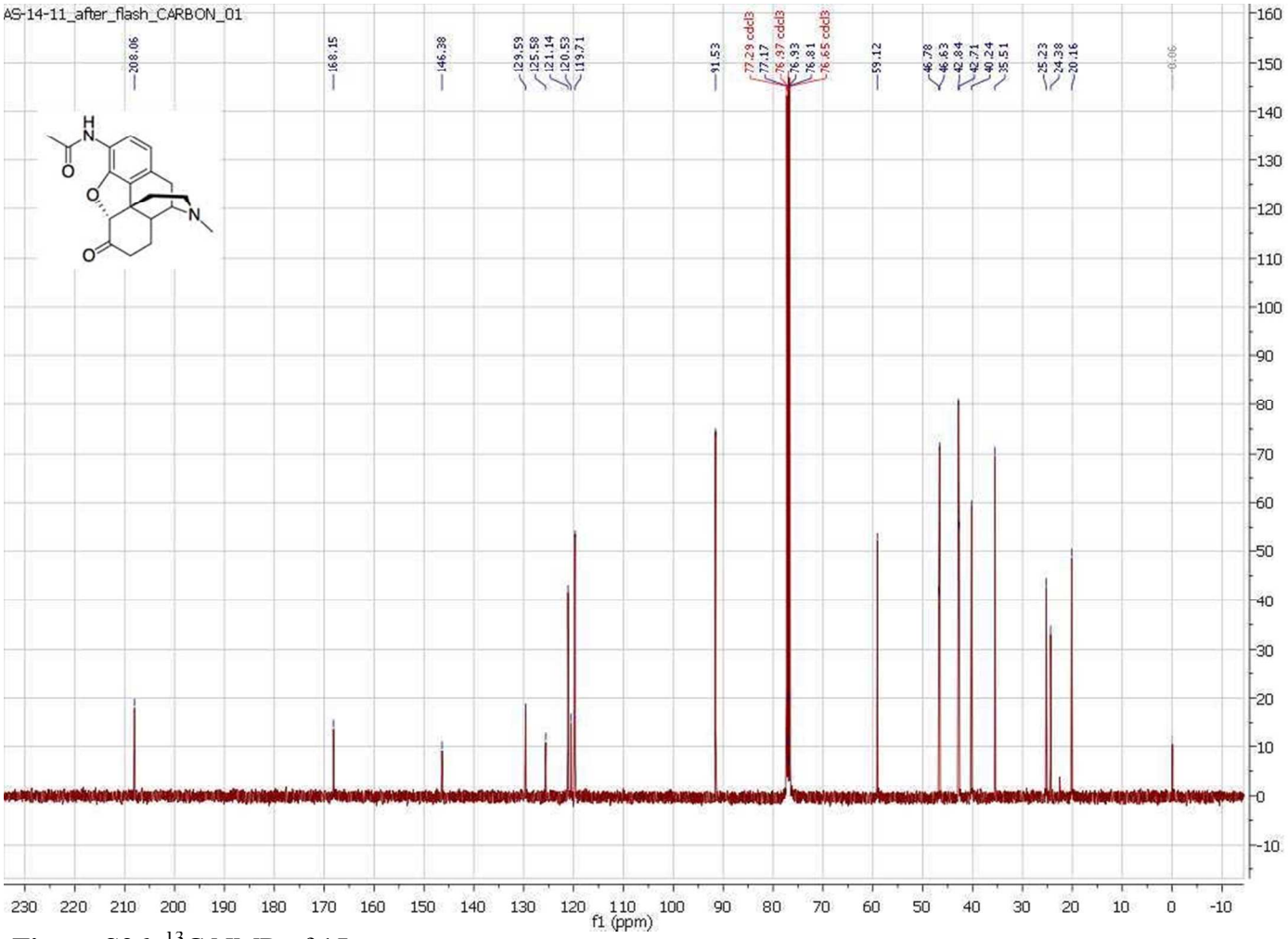

Figure S26. ^{13}C NMR of **15**

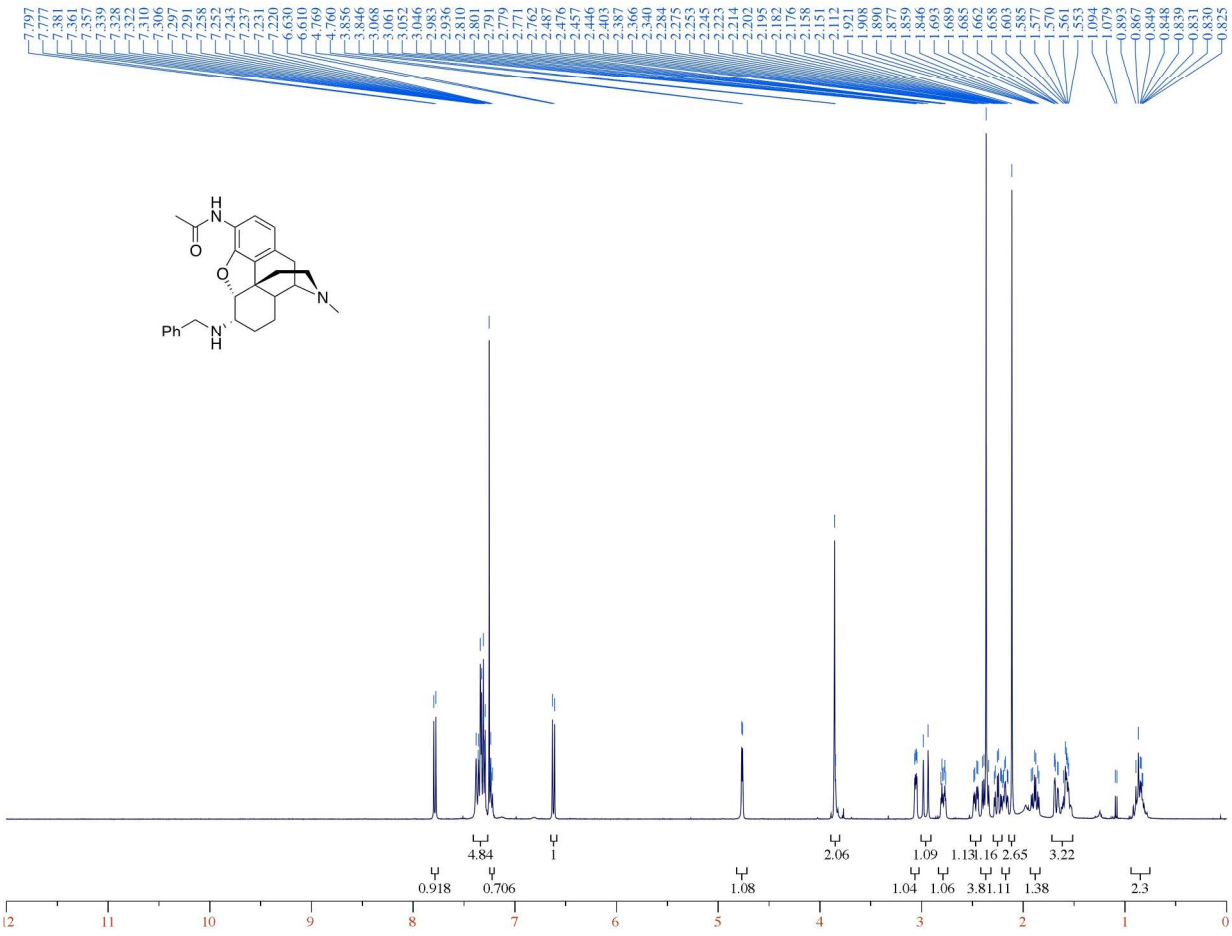

Figure S27. ^{1}H NMR of **16**

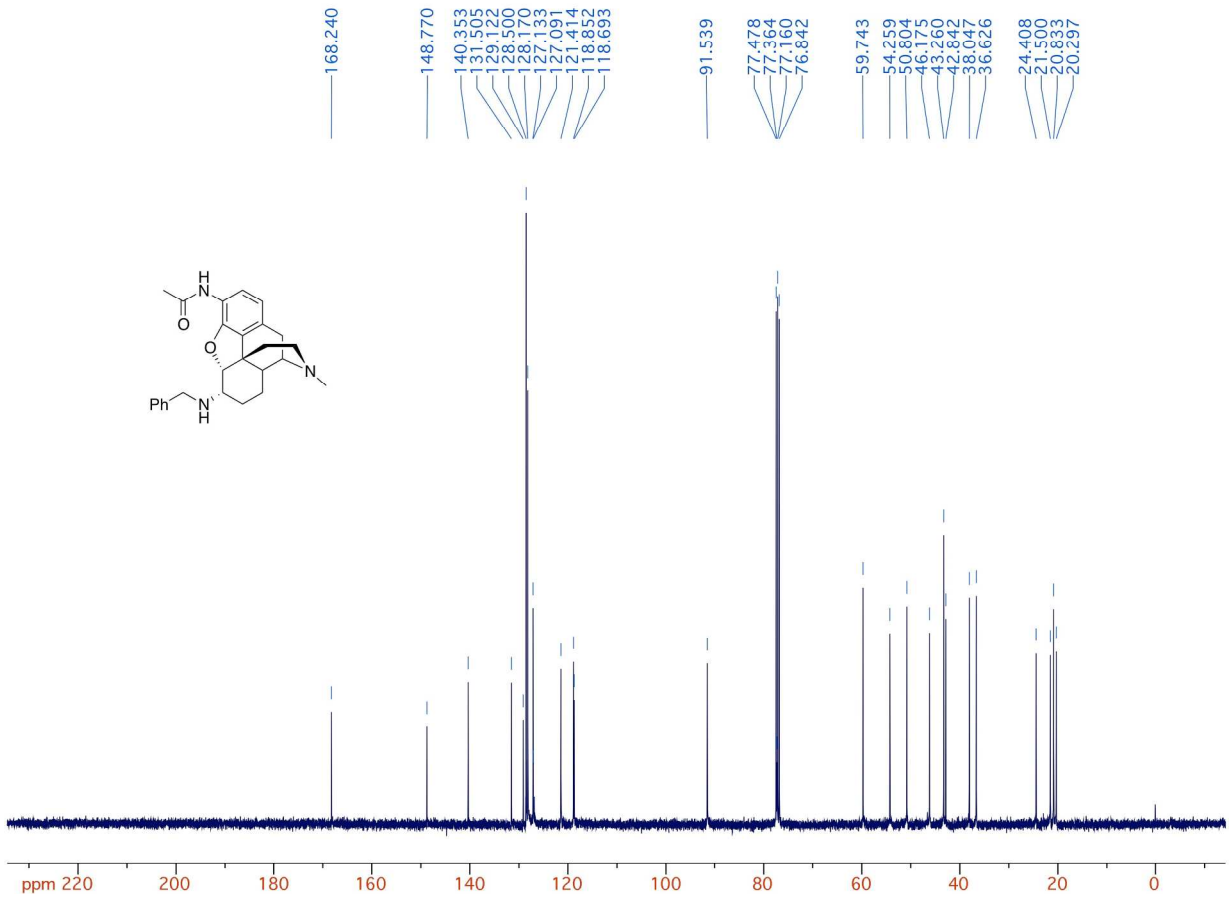

Figure S28. ^{13}C NMR of **16**

Table S1. Affinity of 1 and 3 induced antibodies (IC_{50}; μM) for individual mice measured using competition ELISA[a]

Mice Group	Mice ID	Heroin and its metabolites						Other abused prescription opioid drugs										
		Heroin	6-AM	Morphine	M-3G	M-6G	Normorphine	Codeine	Oxycodone	Hydrocodone	Oxymorphone	Hydromorphone	Levorphanol	Meperidine	Tramadol	Fentanyl	Sufentanil	Nalbuphine
TT-3 + ALF	Pooled sera	>1000	41.64	2.87	>1000	312.50	18.37	>1000	>1000	>1000	66.26	13.54	3.42	>1000	>1000	>1000	>1000	>1000
	251	>1000	164.40	28.05	>1000	242.10	14.98	>1000	>1000	>1000	69.70	100.50	3.52	>1000	>1000	>1000	>1000	>1000
	252	>1000	124.50	29.87	>1000	190.70	13.98	>1000	>1000	>1000	167.80	40.46	7.16	>1000	>1000	>1000	>1000	>1000
	253	332.40	14.26	3.89	>1000	184.20	9.09	>1000	>1000	>1000	35.22	27.58	0.50	>1000	>1000	>1000	>1000	>1000
	254	>1000	143.20	31.72	>1000	804.60	33.26	>1000	>1000	>1000	127.30	101.30	4.58	>1000	>1000	>1000	>1000	>1000
	255	>1000	124.70	37.65	>1000	968.50	27.55	>1000	>1000	>1000	290.30	23.74	51.40	>1000	>1000	>1000	>1000	>1000
	256	>1000	153.10	50.63	>1000	222.50	24.89	>1000	>1000	>1000	129.80	22.23	4.46	>1000	>1000	>1000	>1000	901.80
	257	>1000	55.53	6.42	>1000	349.70	21.84	>1000	>1000	>1000	103.40	207.70	12.04	>1000	>1000	>1000	>1000	>1000
	258	>1000	77.22	21.00	>1000	>1000	23.26	>1000	>1000	>1000	102.10	20.57	10.60	>1000	>1000	>1000	>1000	>1000
	259	>1000	97.63	20.70	>1000	322.20	18.44	>1000	>1000	>1000	44.48	37.83	1.30	>1000	>1000	>1000	>1000	>1000
	260	>1000	89.24	13.34	>1000	414.50	9.60	>1000	>1000	>1000	33.58	15.40	1.38	>1000	>1000	>1000	>1000	>1000
TT-1 + ALF	Pooled sera	1.58	1.86	0.71	2.89	1.04	111.20	6.56	496.00	0.88	81.88	0.95	2.84	268.80	>1000	>1000	>1000	>1000
	311	1.91	7.35	3.21	0.39	0.69	73.84	3.04	416.40	1.96	108.90	2.72	0.70	265.00	>1000	>1000	>1000	>1000
	312	2.61	7.00	7.62	6.85	5.34	196.40	10.30	824.10	5.60	213.80	2.99	6.88	>1000	>1000	>1000	>1000	>1000
	313	1.07	2.00	1.09	2.53	1.44	39.82	0.34	134.40	1.60	75.55	2.60	0.87	191.00	>1000	>1000	>1000	>1000
	314	3.62	5.47	2.50	6.74	2.97	133.50	1.58	618.10	6.91	54.57	5.00	2.36	75.87	>1000	>1000	>1000	>1000
	315	0.60	1.98	2.93	10.01	5.93	267.80	12.36	986.20	18.04	349.20	10.25	8.83	>1000	>1000	>1000	>1000	>1000
	316	1.02	4.39	1.80	13.48	2.94	107.90	3.32	647.10	5.75	84.48	3.40	2.59	553.70	>1000	887.10	>1000	>1000
	317	0.50	3.38	2.40	48.50	23.99	99.09	3.12	560.20	2.68	104.80	3.02	1.38	264.20	>1000	>1000	>1000	>1000
	318	0.42	1.33	0.64	29.25	19.36	60.94	0.59	273.90	2.60	74.86	1.68	3.51	416.90	>1000	>1000	>1000	>1000
	319	0.49	2.77	0.65	43.32	114.20	62.28	2.76	410.90	3.39	69.13	2.87	6.10	335.40	>1000	>1000	>1000	>1000
	320	0.42	1.56	0.72	118.70	72.90	82.75	0.56	474.60	2.03	119.60	1.40	0.67	469.80	>1000	>1000	>1000	>1000

[a] Values denote IC_{50} for the indicated drugs (μM) measured from triplicate measurements using competition ELISA from pooled and individual mice sera from each group (n=10). IC_{50} was defined as the drug concentration that produced 50% inhibition of maximal antibody and hapten binding as calculated from normalized competition curves using log(inhibitor) vs. normalized response-variable slope regression. The Mean ± SEM of IC_{50} values for all drugs from each mice group are shown in Table 2.

Table S2. Affinity of 1 induced antibodies (IC_{50}; μM) for individual rats measured using competition ELISA[a]

Rat Group	Rat ID	Heroin and its metabolites						Other abused prescription opioid drugs										
		Heroin	6-AM	Morphine	M-3G	M-6G	Normorphine	Codeine	Oxycodone	Hydrocodone	Oxymorphone	Hydromorphone	Levorphanol	Meperidine	Tramadol	Fentanyl	Sufentanil	Nalbuphine
TT-1 + ALF	Pooled sera	2.64	2.36	11.44	16.41	71.15	226.70	12.78	56.08	10.12	136.80	25.85	36.12	>1000	>1000	>1000	>1000	>1000
	475	1.14	0.91	7.16	7.21	14.23	457.40	2.01	25.32	4.57	23.36	6.97	6.92	>1000	>1000	>1000	>1000	>1000
	476	1.71	0.75	1.72	13.12	16.06	93.87	7.31	231.90	14.47	273.70	14.86	44.72	282.10	>1000	>1000	>1000	>1000
	477	3.12	1.26	7.55	22.08	33.12	21.84	14.05	33.54	21.38	81.81	27.05	24.22	>1000	>1000	>1000	>1000	>1000
	478	5.32	0.90	5.73	56.90	205.80	123.20	33.24	52.90	23.58	85.17	23.24	31.17	>1000	>1000	>1000	>1000	>1000
	479	5.36	5.66	25.03	130.90	390.80	287.10	46.84	532.30	20.69	849.10	82.85	248.00	>1000	>1000	>1000	>1000	>1000
	480	3.62	0.98	2.30	18.25	49.21	384.70	17.25	143.10	19.63	185.00	15.25	36.50	>1000	>1000	>1000	>1000	>1000
	481	1.50	0.86	5.73	23.23	91.56	107.80	9.50	42.46	5.43	59.85	14.83	18.25	>1000	>1000	>1000	>1000	>1000
	482	2.33	0.69	1.73	12.24	34.61	67.40	7.33	95.22	7.76	178.90	5.61	18.86	>1000	>1000	>1000	>1000	>1000

[a] Values denote IC_{50} for the indicated drugs (μM) measured from triplicate measurements using competition ELISA from pooled and individual rat sera from each group (n=7-8). IC_{50} was defined as the drug concentration that produced 50% inhibition of maximal antibody and hapten binding as calculated from normalized competition curves using log(inhibitor) vs. normalized response-variable slope regression. The Mean ± SEM of IC_{50} values for all drugs from the rat group are shown in Table 2.

Table S3. Microanalysis (CHN)

	Calculated				Found		
Compound	For	C	H	N	C	H	N
1	$C_{41}H_{43}N_3O_3S$•*t*BuOH	73.84	7.39	5.74	73.63	7.39	5.97
15	$C_{19}H_{22}O_3N_2$•oxalic acid•H_2O	58.06	6.03	6.45	58.27	6.16	6.38
16	$C_{26}H_{31}O_2N_3$•1.5 oxalic acid• 2 H_2O•0.5 CH_3OH	58.60	6.67	6.95	58.44	6.67	6.81
19	$C_{24}H_{33}N_3O_4$	67.42	7.78	9.83	67.04	7.73	9.77

Information on X-ray crystal structure deposition

The structures of **19** and **20** were solved and refined with the aid of the program SHELXTL (Bruker). The coordinates for **19** and **20** were deposited at Cambridge Crystallographic Data Centre with deposition numbers CCDC 1553894 and CCDC 1553895, respectively.

Table S4. Crystal data and structure refinement for **19**

Empirical formula	$C_{24}H_{33}N_3O_4$	
Formula weight	427.53	
Temperature	149(2) K	
Wavelength	1.54178 Å	
Crystal system	Monoclinic	
Space group	$P2_1$	
Unit cell dimensions	a = 9.5456(4) Å	α= 90°.
	b = 7.6635(3) Å	β= 97.0255(19)°.
	c = 15.7025(6) Å	γ = 90°.
Volume	1140.06(8) $Å^3$	
Z	2	
Density (150K)	1.245 Mg/m^3	
Absorption coefficient	0.687 mm^{-1}	
F(000)	460	
Crystal size	0.523 x 0.456 x 0.147 mm^3	
θ range for data collection	4.667 to 72.200°.	
Index ranges	-9<=h<=11, -7<=k<=9, -18<=l<=18	
Reflections collected	7047	
Independent reflections	3615 [R(int) = 0.0272]	
Completeness to θ = 67.679°	94.7 %	
Absorption correction	Semi-empirical from equivalents	
Max. and min. transmission	0.7536 and 0.6377	
Refinement method	Full-matrix least-squares on F^2	
Data / restraints / parameters	3615 / 1 / 286	
Goodness-of-fit on F^2	1.011	
Final R indices [I>2σ(I)]	R1 = 0.0311, wR2 = 0.0853	
R indices (all data)	R1 = 0.0323, wR2 = 0.0861	
Absolute structure parameter	0.08(6)	
Extinction coefficient	0.0052(13)	
Largest diff. peak and hole	0.224 and -0.152 $e.Å^{-3}$	

Table S5. Atomic coordinates (x 10^4) and equivalent isotropic displacement parameters ($Å^2$x10^3) for **19**. U(eq) is defined as one third of the trace of the orthogonalized U^{ij} tensor

	x	y	z	U(eq)
C(1)	4610(2)	-3771(3)	2807(1)	26(1)
C(2)	4864(2)	-2215(3)	2405(1)	26(1)
C(3)	4113(2)	-681(3)	2526(1)	24(1)
C(4)	3140(2)	-780(3)	3113(1)	21(1)
O(5)	2239(1)	516(2)	3310(1)	24(1)
C(5)	1109(2)	-351(3)	3711(1)	23(1)
C(6)	-170(2)	-660(3)	3036(1)	26(1)
C(7)	-48(2)	-2350(3)	2531(1)	29(1)
C(8)	62(2)	-3974(3)	3109(1)	32(1)
C(9)	1834(2)	-5249(3)	4318(1)	23(1)
C(10)	3062(2)	-5510(3)	3753(1)	27(1)
C(11)	3580(2)	-3857(3)	3381(1)	23(1)
C(12)	2928(2)	-2314(3)	3537(1)	20(1)
C(13)	1774(2)	-2061(3)	4101(1)	21(1)
C(14)	851(2)	-3700(3)	4018(1)	23(1)
C(15)	2383(2)	-1820(3)	5050(1)	25(1)
C(16)	3169(2)	-3437(3)	5412(1)	26(1)
N(17)	2300(2)	-5006(2)	5242(1)	24(1)
C(17)	3023(2)	-6530(3)	5640(2)	31(1)
N(18)	4360(2)	860(2)	2062(1)	27(1)
C(19)	3342(2)	1692(3)	1550(1)	26(1)
O(19)	2079(1)	1365(2)	1480(1)	37(1)
O(20)	3936(1)	2965(2)	1117(1)	28(1)
C(21)	3077(2)	4040(3)	476(1)	30(1)
C(22)	2082(3)	5195(4)	912(2)	40(1)
C(23)	2299(3)	2925(4)	-223(2)	43(1)
C(24)	4216(3)	5137(4)	128(2)	43(1)
N(25)	-339(2)	843(3)	2458(1)	30(1)
C(26)	-1595(2)	1478(3)	2141(1)	26(1)
O(26)	-2705(2)	930(3)	2361(1)	43(1)
C(27)	-1585(2)	2938(3)	1493(2)	33(1)

Table S6. Bond lengths [Å] and angles [°] for **19**

C(1)-C(2)	1.385(3)	C(1)-C(11)	1.414(3)
C(1)-H(1A)	0.9500	C(2)-C(3)	1.402(3)
C(2)-H(2A)	0.9500	C(3)-C(4)	1.388(2)
C(3)-N(18)	1.422(3)	C(4)-O(5)	1.373(2)
C(4)-C(12)	1.378(3)	O(5)-C(5)	1.473(2)
C(5)-C(6)	1.534(3)	C(5)-C(13)	1.549(3)
C(5)-H(5A)	1.0000	C(6)-N(25)	1.462(3)
C(6)-C(7)	1.530(3)	C(6)-H(6A)	1.0000
C(7)-C(8)	1.535(3)	C(7)-H(7A)	0.9900
C(7)-H(7B)	0.9900	C(8)-C(14)	1.545(3)
C(8)-H(8A)	0.9900	C(8)-H(8B)	0.9900
C(9)-N(17)	1.477(3)	C(9)-C(14)	1.549(3)
C(9)-C(10)	1.566(2)	C(9)-H(9A)	1.0000
C(10)-C(11)	1.504(3)	C(10)-H(10A)	0.9900
C(10)-H(10B)	0.9900	C(11)-C(12)	1.372(3)
C(12)-C(13)	1.508(2)	C(13)-C(14)	1.531(3)
C(13)-C(15)	1.544(3)	C(14)-H(14A)	1.0000
C(15)-C(16)	1.522(3)	C(15)-H(15A)	0.9900
C(15)-H(15B)	0.9900	C(16)-N(17)	1.466(3)
C(16)-H(16A)	0.9900	C(16)-H(16B)	0.9900
N(17)-C(17)	1.459(3)	C(17)-H(17A)	0.9800
C(17)-H(17B)	0.9800	C(17)-H(17C)	0.9800
N(18)-C(19)	1.344(3)	N(18)-H(18A)	0.8800
C(19)-O(19)	1.223(2)	C(19)-O(20)	1.352(2)
O(20)-C(21)	1.471(3)	C(21)-C(23)	1.513(4)
C(21)-C(22)	1.520(3)	C(21)-C(24)	1.527(3)
C(22)-H(22A)	0.9800	C(22)-H(22B)	0.9800
C(22)-H(22C)	0.9800	C(23)-H(23A)	0.9800
C(23)-H(23B)	0.9800	C(23)-H(23C)	0.9800
C(24)-H(24A)	0.9800	C(24)-H(24B)	0.9800
C(24)-H(24C)	0.9800	N(25)-C(26)	1.333(3)
N(25)-H(25A)	0.8800	C(26)-O(26)	1.228(2)
C(26)-C(27)	1.513(3)	C(27)-H(27A)	0.9800
C(27)-H(27B)	0.9800	C(27)-H(27C)	0.9800
C(2)-C(1)-C(11)	120.33(18)	C(2)-C(1)-H(1A)	119.8
C(11)-C(1)-H(1A)	119.8	C(1)-C(2)-C(3)	122.60(16)
C(1)-C(2)-H(2A)	118.7	C(3)-C(2)-H(2A)	118.7
C(4)-C(3)-C(2)	116.06(18)	C(4)-C(3)-N(18)	123.49(19)
C(2)-C(3)-N(18)	120.44(16)	O(5)-C(4)-C(12)	112.00(15)
O(5)-C(4)-C(3)	126.76(18)	C(12)-C(4)-C(3)	121.14(18)
C(4)-O(5)-C(5)	106.38(14)	O(5)-C(5)-C(6)	109.64(15)
O(5)-C(5)-C(13)	105.33(14)	C(6)-C(5)-C(13)	113.29(16)
O(5)-C(5)-H(5A)	109.5	C(6)-C(5)-H(5A)	109.5

Table S6. (continued)

C(13)-C(5)-H(5A)	109.5	N(25)-C(6)-C(7)	110.81(16)
N(25)-C(6)-C(5)	109.00(16)	C(7)-C(6)-C(5)	112.58(16)
N(25)-C(6)-H(6A)	108.1	C(7)-C(6)-H(6A)	108.1
C(5)-C(6)-H(6A)	108.1	C(6)-C(7)-C(8)	112.60(16)
C(6)-C(7)-H(7A)	109.1	C(8)-C(7)-H(7A)	109.1
C(6)-C(7)-H(7B)	109.1	C(8)-C(7)-H(7B)	109.1
H(7A)-C(7)-H(7B)	107.8	C(7)-C(8)-C(14)	115.21(18)
C(7)-C(8)-H(8A)	108.5	C(14)-C(8)-H(8A)	108.5
C(7)-C(8)-H(8B)	108.5	C(14)-C(8)-H(8B)	108.5
H(8A)-C(8)-H(8B)	107.5	N(17)-C(9)-C(14)	107.49(16)
N(17)-C(9)-C(10)	114.55(16)	C(14)-C(9)-C(10)	113.15(15)
N(17)-C(9)-H(9A)	107.1	C(14)-C(9)-H(9A)	107.1
C(10)-C(9)-H(9A)	107.1	C(11)-C(10)-C(9)	114.62(16)
C(11)-C(10)-H(10A)	108.6	C(9)-C(10)-H(10A)	108.6
C(11)-C(10)-H(10B)	108.6	C(9)-C(10)-H(10B)	108.6
H(10A)-C(10)-H(10B)	107.6	C(12)-C(11)-C(1)	116.10(18)
C(12)-C(11)-C(10)	118.59(15)	C(1)-C(11)-C(10)	125.02(18)
C(11)-C(12)-C(4)	123.50(16)	C(11)-C(12)-C(13)	126.55(17)
C(4)-C(12)-C(13)	109.59(16)	C(12)-C(13)-C(14)	107.37(16)
C(12)-C(13)-C(15)	111.53(15)	C(14)-C(13)-C(15)	108.99(15)
C(12)-C(13)-C(5)	99.81(14)	C(14)-C(13)-C(5)	117.19(15)
C(15)-C(13)-C(5)	111.57(16)	C(13)-C(14)-C(8)	113.62(16)
C(13)-C(14)-C(9)	106.38(15)	C(8)-C(14)-C(9)	112.69(17)
C(13)-C(14)-H(14A)	108.0	C(8)-C(14)-H(14A)	108.0
C(9)-C(14)-H(14A)	108.0	C(16)-C(15)-C(13)	111.86(16)
C(16)-C(15)-H(15A)	109.2	C(13)-C(15)-H(15A)	109.2
C(16)-C(15)-H(15B)	109.2	C(13)-C(15)-H(15B)	109.2
H(15A)-C(15)-H(15B)	107.9	N(17)-C(16)-C(15)	110.96(16)
N(17)-C(16)-H(16A)	109.4	C(15)-C(16)-H(16A)	109.4
N(17)-C(16)-H(16B)	109.4	C(15)-C(16)-H(16B)	109.4
H(16A)-C(16)-H(16B)	108.0	C(17)-N(17)-C(16)	110.55(16)
C(17)-N(17)-C(9)	112.99(17)	C(16)-N(17)-C(9)	112.21(15)
N(17)-C(17)-H(17A)	109.5	N(17)-C(17)-H(17B)	109.5
H(17A)-C(17)-H(17B)	109.5	N(17)-C(17)-H(17C)	109.5
H(17A)-C(17)-H(17C)	109.5	H(17B)-C(17)-H(17C)	109.5
C(19)-N(18)-C(3)	123.20(16)	C(19)-N(18)-H(18A)	118.4
C(3)-N(18)-H(18A)	118.4	O(19)-C(19)-N(18)	126.11(18)
O(19)-C(19)-O(20)	124.86(19)	N(18)-C(19)-O(20)	109.03(16)
C(19)-O(20)-C(21)	121.04(15)	O(20)-C(21)-C(23)	111.3(2)
O(20)-C(21)-C(22)	110.15(17)	C(23)-C(21)-C(22)	112.18(19)
O(20)-C(21)-C(24)	101.07(17)	C(23)-C(21)-C(24)	110.99(19)
C(22)-C(21)-C(24)	110.6(2)	C(21)-C(22)-H(22A)	109.5
C(21)-C(22)-H(22B)	109.5	H(22A)-C(22)-H(22B)	109.5

Table S6. (continued)

C(21)-C(22)-H(22C)	109.5	H(22A)-C(22)-H(22C)	109.5
H(22B)-C(22)-H(22C)	109.5	C(21)-C(23)-H(23A)	109.5
C(21)-C(23)-H(23B)	109.5	H(23A)-C(23)-H(23B)	109.5
C(21)-C(23)-H(23C)	109.5	H(23A)-C(23)-H(23C)	109.5
H(23B)-C(23)-H(23C)	109.5	C(21)-C(24)-H(24A)	109.5
C(21)-C(24)-H(24B)	109.5	H(24A)-C(24)-H(24B)	109.5
C(21)-C(24)-H(24C)	109.5	H(24A)-C(24)-H(24C)	109.5
H(24B)-C(24)-H(24C)	109.5	C(26)-N(25)-C(6)	123.09(16)
C(26)-N(25)-H(25A)	118.5	C(6)-N(25)-H(25A)	118.5
O(26)-C(26)-N(25)	122.5(2)	O(26)-C(26)-C(27)	121.22(18)
N(25)-C(26)-C(27)	116.27(17)	C(26)-C(27)-H(27A)	109.5
C(26)-C(27)-H(27B)	109.5	H(27A)-C(27)-H(27B)	109.5
C(26)-C(27)-H(27C)	109.5	H(27A)-C(27)-H(27C)	109.5
H(27B)-C(27)-H(27C)	109.5		

Table S7. Anisotropic displacement parameters ($Å^2 x\ 10^3$) for **19**. The anisotropic displacement factor exponent takes the form: $-2\ \pi^2[h^2 a^{*2} U^{11} + ... + 2\ h\ k\ a^*\ b^*\ U^{12}]$

	U^{11}	U^{22}	U^{33}	U^{23}	U^{13}	U^{12}
C(1)	26(1)	26(1)	26(1)	-3(1)	5(1)	4(1)
C(2)	22(1)	34(1)	23(1)	0(1)	4(1)	0(1)
C(3)	19(1)	27(1)	25(1)	5(1)	-1(1)	-4(1)
C(4)	17(1)	21(1)	25(1)	-1(1)	-2(1)	-3(1)
O(5)	20(1)	19(1)	33(1)	4(1)	4(1)	-1(1)
C(5)	22(1)	21(1)	28(1)	2(1)	7(1)	1(1)
C(6)	18(1)	28(1)	32(1)	9(1)	5(1)	1(1)
C(7)	26(1)	32(1)	27(1)	3(1)	-5(1)	-5(1)
C(8)	32(1)	27(1)	33(1)	2(1)	-7(1)	-8(1)
C(9)	25(1)	18(1)	27(1)	2(1)	4(1)	-4(1)
C(10)	35(1)	18(1)	29(1)	-1(1)	7(1)	1(1)
C(11)	25(1)	21(1)	21(1)	-1(1)	0(1)	0(1)
C(12)	20(1)	21(1)	20(1)	-1(1)	0(1)	-2(1)
C(13)	22(1)	20(1)	22(1)	0(1)	2(1)	1(1)
C(14)	22(1)	22(1)	25(1)	4(1)	1(1)	-3(1)
C(15)	28(1)	24(1)	24(1)	-2(1)	4(1)	0(1)
C(16)	26(1)	30(1)	22(1)	0(1)	1(1)	-2(1)
N(17)	24(1)	24(1)	24(1)	6(1)	2(1)	1(1)
C(17)	28(1)	30(1)	34(1)	10(1)	3(1)	4(1)
N(18)	14(1)	32(1)	34(1)	12(1)	1(1)	-4(1)
C(19)	21(1)	33(1)	25(1)	6(1)	3(1)	-2(1)
O(19)	18(1)	52(1)	38(1)	18(1)	0(1)	-4(1)
O(20)	21(1)	33(1)	29(1)	12(1)	2(1)	0(1)
C(21)	30(1)	34(1)	26(1)	9(1)	2(1)	4(1)
C(22)	36(1)	42(1)	41(1)	5(1)	2(1)	9(1)
C(23)	44(1)	53(2)	30(1)	5(1)	-3(1)	4(1)
C(24)	42(1)	44(2)	44(1)	21(1)	12(1)	1(1)
N(25)	17(1)	31(1)	42(1)	14(1)	6(1)	1(1)
C(26)	19(1)	28(1)	31(1)	1(1)	0(1)	-1(1)
O(26)	17(1)	59(1)	53(1)	22(1)	1(1)	-1(1)
C(27)	29(1)	29(1)	38(1)	6(1)	-8(1)	-3(1)

Table S8. Hydrogen coordinates (x 10^4) and isotropic displacement parameters ($Å^2$x 10^3) for **19**

	x	y	z	U(eq)
H(1A)	5130	-4787	2697	31
H(2A)	5576	-2186	2032	32
H(5A)	824	403	4180	28
H(6A)	-1030	-744	3339	31
H(7A)	798	-2285	2225	35
H(7B)	-885	-2465	2096	35
H(8A)	547	-4905	2821	38
H(8B)	-904	-4391	3164	38
H(9A)	1244	-6330	4259	28
H(10A)	3864	-6076	4108	32
H(10B)	2736	-6315	3277	32
H(14A)	131	-3589	4426	28
H(15A)	3036	-811	5101	30
H(15B)	1603	-1561	5393	30
H(16A)	4053	-3569	5148	31
H(16B)	3423	-3299	6038	31
H(17A)	3185	-6364	6264	46
H(17B)	3930	-6681	5417	46
H(17C)	2439	-7570	5508	46
H(18A)	5221	1289	2113	32
H(22A)	1399	4464	1166	60
H(22B)	1579	5982	488	60
H(22C)	2626	5882	1364	60
H(23A)	1583	2226	16	64
H(23B)	2970	2149	-460	64
H(23C)	1842	3678	-680	64
H(24A)	4854	4371	-143	64
H(24B)	4753	5776	601	64
H(24C)	3772	5967	-297	64
H(25A)	424	1351	2314	36
H(27A)	-2551	3160	1226	50
H(27B)	-996	2602	1051	50
H(27C)	-1203	3998	1783	50

—

Table S9. Torsion angles [°] for **19**

C(11)-C(1)-C(2)-C(3)	-1.3(3)	C(1)-C(2)-C(3)-C(4)	3.3(3)
C(1)-C(2)-C(3)-N(18)	-176.52(19)	C(2)-C(3)-C(4)-O(5)	-176.76(19)
N(18)-C(3)-C(4)-O(5)	3.0(3)	C(2)-C(3)-C(4)-C(12)	-0.7(3)
N(18)-C(3)-C(4)-C(12)	179.06(18)	C(12)-C(4)-O(5)-C(5)	-15.8(2)
C(3)-C(4)-O(5)-C(5)	160.54(19)	C(4)-O(5)-C(5)-C(6)	-96.68(17)
C(4)-O(5)-C(5)-C(13)	25.54(19)	O(5)-C(5)-C(6)-N(25)	-38.3(2)
C(13)-C(5)-C(6)-N(25)	-155.65(15)	O(5)-C(5)-C(6)-C(7)	85.06(18)
C(13)-C(5)-C(6)-C(7)	-32.3(2)	N(25)-C(6)-C(7)-C(8)	-177.29(17)
C(5)-C(6)-C(7)-C(8)	60.4(2)	C(6)-C(7)-C(8)-C(14)	-33.4(2)
N(17)-C(9)-C(10)-C(11)	-92.0(2)	C(14)-C(9)-C(10)-C(11)	31.7(2)
C(2)-C(1)-C(11)-C(12)	-3.2(3)	C(2)-C(1)-C(11)-C(10)	170.5(2)
C(9)-C(10)-C(11)-C(12)	-2.0(3)	C(9)-C(10)-C(11)-C(1)	-175.56(19)
C(1)-C(11)-C(12)-C(4)	5.8(3)	C(10)-C(11)-C(12)-C(4)	-168.30(19)
C(1)-C(11)-C(12)-C(13)	178.29(18)	C(10)-C(11)-C(12)-C(13)	4.2(3)
O(5)-C(4)-C(12)-C(11)	172.58(17)	C(3)-C(4)-C(12)-C(11)	-4.0(3)
O(5)-C(4)-C(12)-C(13)	-1.0(2)	C(3)-C(4)-C(12)-C(13)	-177.56(17)
C(11)-C(12)-C(13)-C(14)	-34.6(3)	C(4)-C(12)-C(13)-C(14)	138.74(17)
C(11)-C(12)-C(13)-C(15)	84.7(2)	C(4)-C(12)-C(13)-C(15)	-101.92(19)
C(11)-C(12)-C(13)-C(5)	-157.27(19)	C(4)-C(12)-C(13)-C(5)	16.06(19)
O(5)-C(5)-C(13)-C(12)	-24.55(18)	C(6)-C(5)-C(13)-C(12)	95.28(17)
O(5)-C(5)-C(13)-C(14)	-139.99(16)	C(6)-C(5)-C(13)-C(14)	-20.2(2)
O(5)-C(5)-C(13)-C(15)	93.40(17)	C(6)-C(5)-C(13)-C(15)	-146.77(15)
C(12)-C(13)-C(14)-C(8)	-64.9(2)	C(15)-C(13)-C(14)-C(8)	174.15(16)
C(5)-C(13)-C(14)-C(8)	46.3(2)	C(12)-C(13)-C(14)-C(9)	59.66(19)
C(15)-C(13)-C(14)-C(9)	-61.29(18)	C(5)-C(13)-C(14)-C(9)	170.84(16)
C(7)-C(8)-C(14)-C(13)	-18.0(2)	C(7)-C(8)-C(14)-C(9)	-139.06(18)
N(17)-C(9)-C(14)-C(13)	65.95(17)	C(10)-C(9)-C(14)-C(13)	-61.5(2)
N(17)-C(9)-C(14)-C(8)	-168.92(15)	C(10)-C(9)-C(14)-C(8)	63.6(2)
C(12)-C(13)-C(15)-C(16)	-63.6(2)	C(14)-C(13)-C(15)-C(16)	54.8(2)
C(5)-C(13)-C(15)-C(16)	-174.22(15)	C(13)-C(15)-C(16)-N(17)	-51.0(2)
C(15)-C(16)-N(17)-C(17)	-176.13(16)	C(15)-C(16)-N(17)-C(9)	56.7(2)
C(14)-C(9)-N(17)-C(17)	169.53(15)	C(10)-C(9)-N(17)-C(17)	-63.8(2)
C(14)-C(9)-N(17)-C(16)	-64.66(19)	C(10)-C(9)-N(17)-C(16)	62.0(2)
C(4)-C(3)-N(18)-C(19)	-57.7(3)	C(2)-C(3)-N(18)-C(19)	122.1(2)
C(3)-N(18)-C(19)-O(19)	7.8(3)	C(3)-N(18)-C(19)-O(20)	-172.20(18)
O(19)-C(19)-O(20)-C(21)	-2.9(3)	N(18)-C(19)-O(20)-C(21)	177.10(18)
C(19)-O(20)-C(21)-C(23)	-57.5(2)	C(19)-O(20)-C(21)-C(22)	67.6(3)
C(19)-O(20)-C(21)-C(24)	-175.43(19)	C(7)-C(6)-N(25)-C(26)	93.2(2)
C(5)-C(6)-N(25)-C(26)	-142.4(2)	C(6)-N(25)-C(26)-O(26)	5.7(4)
C(6)-N(25)-C(26)-C(27)	-174.88(19)		

Table S10. Hydrogen bonds for **19** [Å and °]

D-H...A	d(D-H)	d(H...A)	d(D...A)	<(DHA)
N(18)-H(18A)...O(26)#1	0.88	1.99	2.784(2)	149.6
N(25)-H(25A)...O(19)	0.88	2.17	2.953(2)	147.5

Symmetry transformations used to generate equivalent atoms:
#1 x+1,y,z

Table S11. Crystal data and structure refinement for **20**

Empirical formula	$C_{26}H_{42}ClN_3O_5$	
Formula weight	512.07	
Temperature	150(2) K	
Wavelength	1.54178 Å	
Crystal system	Monoclinic	
Space group	C2	
Unit cell dimensions	a = 14.8766(8) Å	α = 90°.
	b = 9.9184(5) Å	β = 105.562(2)°.
	c = 19.7465(10) Å	γ = 90°.
Volume	2806.8(3) $Å^3$	
Z	4	
Density (150K)	1.212 Mg/m^3	
Absorption coefficient	1.517 mm^{-1}	
F(000)	1104	
Crystal size	0.214 x 0.115 x 0.030 mm^3	
θ range for data collection	4.649 to 74.509°.	
Index ranges	-16<=h<=18, -9<=k<=11, -23<=l<=21	
Reflections collected	8951	
Independent reflections	3980 [R(int) = 0.0194]	
Completeness to θ = 67.679°	93.9 %	
Absorption correction	Semi-empirical from equivalents	
Max. and min. transmission	0.7538 and 0.6782	
Refinement method	Full-matrix least-squares on F^2	
Data / restraints / parameters	3980 / 3 / 328	
Goodness-of-fit on F^2	1.044	
Final R indices [I>2σ(I)]	R1 = 0.0300, wR2 = 0.0794	
R indices (all data)	R1 = 0.0313, wR2 = 0.0807	
Absolute structure parameter	0.056(6)	
Largest diff. peak and hole	0.246 and -0.291 $e.Å^{-3}$	

Table S12. Atomic coordinates (x 10^4) and equivalent isotropic displacement parameters ($Å^2$x10^3) for **20**. U(eq) is defined as one third of the trace of the orthogonalized U^{ij} tensor

	x	y	z	U(eq)
C(1)	7973(2)	7985(3)	8065(1)	34(1)
C(2)	8052(2)	7408(3)	7449(1)	32(1)
C(3)	7332(2)	6611(2)	7051(1)	27(1)
O(4)	5809(1)	5651(2)	6895(1)	34(1)
C(4)	6532(2)	6400(2)	7281(1)	26(1)
C(5)	5072(2)	5384(2)	8051(1)	29(1)
C(6)	5605(2)	4191(2)	8464(1)	33(1)
C(7)	5936(2)	4489(3)	9250(1)	40(1)
C(8)	6434(2)	5841(3)	9405(1)	34(1)
C(9)	6254(2)	8342(2)	9192(1)	30(1)
C(10)	7170(2)	8447(3)	8988(1)	36(1)
C(11)	7187(2)	7763(2)	8308(1)	29(1)
C(12)	6463(1)	6935(2)	7927(1)	24(1)
C(13)	5578(1)	6757(2)	8190(1)	25(1)
C(14)	5819(2)	6973(2)	8993(1)	27(1)
C(15)	4882(2)	7872(2)	7846(1)	30(1)
C(16)	5239(2)	9278(3)	8057(1)	35(1)
N(17)	5539(1)	9392(2)	8844(1)	33(1)
C(17)	5821(2)	10788(3)	9085(2)	49(1)
N(18)	7493(1)	5994(2)	6439(1)	30(1)
O(19)	6038(1)	6081(2)	5668(1)	42(1)
C(19)	6876(2)	5857(3)	5803(1)	33(1)
O(20)	7317(1)	5415(2)	5335(1)	40(1)
C(21)	6790(2)	5166(3)	4592(1)	43(1)
C(22)	6096(2)	4041(4)	4549(2)	62(1)
C(23)	7561(2)	4736(4)	4272(2)	56(1)
C(24)	6334(2)	6463(4)	4264(1)	57(1)
N(25)	6387(1)	3764(2)	8196(1)	34(1)
O(26)	5458(2)	2509(2)	7347(1)	57(1)
C(26)	6245(2)	2966(3)	7635(1)	41(1)
C(27)	7079(2)	2657(4)	7373(2)	56(1)
C(1S)	5403(2)	9191(4)	6139(2)	60(1)
C(2S)	4733(2)	10309(4)	5923(2)	56(1)
O(3S)	4389(1)	10762(3)	6492(1)	51(1)
Cl(28)	3602(1)	9294(1)	9064(1)	49(1)

Table S13. Bond lengths [Å] and angles [°] for **20**

C(1)-C(2)	1.377(3)	C(1)-C(11)	1.395(3)
C(1)-H(1)	0.9500	C(2)-C(3)	1.393(3)
C(2)-H(2)	0.9500	C(3)-C(4)	1.399(3)
C(3)-N(18)	1.430(3)	O(4)-C(4)	1.360(3)
O(4)-H(4)	0.822(12)	C(4)-C(12)	1.411(3)
C(5)-C(6)	1.532(3)	C(5)-C(13)	1.545(3)
C(5)-H(5A)	0.9900	C(5)-H(5B)	0.9900
C(6)-N(25)	1.464(3)	C(6)-C(7)	1.526(3)
C(6)-H(6)	1.0000	C(7)-C(8)	1.523(4)
C(7)-H(7A)	0.9900	C(7)-H(7B)	0.9900
C(8)-C(14)	1.536(3)	C(8)-H(8A)	0.9900
C(8)-H(8B)	0.9900	C(9)-C(14)	1.510(3)
C(9)-N(17)	1.515(3)	C(9)-C(10)	1.525(3)
C(9)-H(9)	1.0000	C(10)-C(11)	1.511(3)
C(10)-H(10A)	0.9900	C(10)-H(10B)	0.9900
C(11)-C(12)	1.403(3)	C(12)-C(13)	1.549(3)
C(13)-C(15)	1.542(3)	C(13)-C(14)	1.544(3)
C(14)-H(14)	1.0000	C(15)-C(16)	1.510(4)
C(15)-H(15A)	0.9900	C(15)-H(15B)	0.9900
C(16)-N(17)	1.500(3)	C(16)-H(16A)	0.9900
C(16)-H(16B)	0.9900	N(17)-C(17)	1.488(3)
N(17)-H(17)	1.0000	C(17)-H(17A)	0.9800
C(17)-H(17B)	0.9800	C(17)-H(17C)	0.9800
N(18)-C(19)	1.350(3)	N(18)-H(18)	0.8800
O(19)-C(19)	1.223(3)	C(19)-O(20)	1.342(3)
O(20)-C(21)	1.487(3)	C(21)-C(22)	1.507(5)
C(21)-C(23)	1.511(4)	C(21)-C(24)	1.516(5)
C(22)-H(22A)	0.9800	C(22)-H(22B)	0.9800
C(22)-H(22C)	0.9800	C(23)-H(23A)	0.9800
C(23)-H(23B)	0.9800	C(23)-H(23C)	0.9800
C(24)-H(24A)	0.9800	C(24)-H(24B)	0.9800
C(24)-H(24C)	0.9800	N(25)-C(26)	1.331(3)
N(25)-H(25)	0.8800	O(26)-C(26)	1.242(3)
C(26)-C(27)	1.498(4)	C(27)-H(27A)	0.9800
C(27)-H(27B)	0.9800	C(27)-H(27C)	0.9800
C(1S)-C(2S)	1.476(5)	C(1S)-H(1S)	0.9800
C(1S)-H(2S)	0.9800	C(1S)-H(3S)	0.9800
C(2S)-O(3S)	1.425(3)	C(2S)-H(4S)	0.9900
C(2S)-H(5S)	0.9900	O(3S)-H(6S)	0.822(12)
C(2)-C(1)-C(11)	121.1(2)	C(2)-C(1)-H(1)	119.4
C(11)-C(1)-H(1)	119.4	C(1)-C(2)-C(3)	120.0(2)
C(1)-C(2)-H(2)	120.0	C(3)-C(2)-H(2)	120.0
C(2)-C(3)-C(4)	119.57(19)	C(2)-C(3)-N(18)	116.25(18)

Table S13. (continued)

C(4)-C(3)-N(18)	124.09(19)	C(4)-O(4)-H(4)	110(2)
O(4)-C(4)-C(3)	120.88(18)	O(4)-C(4)-C(12)	118.27(18)
C(3)-C(4)-C(12)	120.84(19)	C(6)-C(5)-C(13)	115.36(18)
C(6)-C(5)-H(5A)	108.4	C(13)-C(5)-H(5A)	108.4
C(6)-C(5)-H(5B)	108.4	C(13)-C(5)-H(5B)	108.4
H(5A)-C(5)-H(5B)	107.5	N(25)-C(6)-C(7)	110.66(19)
N(25)-C(6)-C(5)	112.23(18)	C(7)-C(6)-C(5)	111.8(2)
N(25)-C(6)-H(6)	107.3	C(7)-C(6)-H(6)	107.3
C(5)-C(6)-H(6)	107.3	C(8)-C(7)-C(6)	112.5(2)
C(8)-C(7)-H(7A)	109.1	C(6)-C(7)-H(7A)	109.1
C(8)-C(7)-H(7B)	109.1	C(6)-C(7)-H(7B)	109.1
H(7A)-C(7)-H(7B)	107.8	C(7)-C(8)-C(14)	110.43(19)
C(7)-C(8)-H(8A)	109.6	C(14)-C(8)-H(8A)	109.6
C(7)-C(8)-H(8B)	109.6	C(14)-C(8)-H(8B)	109.6
H(8A)-C(8)-H(8B)	108.1	C(14)-C(9)-N(17)	107.51(18)
C(14)-C(9)-C(10)	110.11(18)	N(17)-C(9)-C(10)	113.69(19)
C(14)-C(9)-H(9)	108.5	N(17)-C(9)-H(9)	108.5
C(10)-C(9)-H(9)	108.5	C(11)-C(10)-C(9)	115.70(19)
C(11)-C(10)-H(10A)	108.4	C(9)-C(10)-H(10A)	108.4
C(11)-C(10)-H(10B)	108.4	C(9)-C(10)-H(10B)	108.4
H(10A)-C(10)-H(10B)	107.4	C(1)-C(11)-C(12)	120.1(2)
C(1)-C(11)-C(10)	116.8(2)	C(12)-C(11)-C(10)	123.0(2)
C(11)-C(12)-C(4)	118.23(19)	C(11)-C(12)-C(13)	119.15(18)
C(4)-C(12)-C(13)	122.33(18)	C(15)-C(13)-C(14)	107.25(17)
C(15)-C(13)-C(5)	108.45(17)	C(14)-C(13)-C(5)	105.84(17)
C(15)-C(13)-C(12)	107.50(17)	C(14)-C(13)-C(12)	110.11(17)
C(5)-C(13)-C(12)	117.28(18)	C(9)-C(14)-C(8)	111.56(19)
C(9)-C(14)-C(13)	110.90(18)	C(8)-C(14)-C(13)	112.57(18)
C(9)-C(14)-H(14)	107.2	C(8)-C(14)-H(14)	107.2
C(13)-C(14)-H(14)	107.2	C(16)-C(15)-C(13)	113.35(18)
C(16)-C(15)-H(15A)	108.9	C(13)-C(15)-H(15A)	108.9
C(16)-C(15)-H(15B)	108.9	C(13)-C(15)-H(15B)	108.9
H(15A)-C(15)-H(15B)	107.7	N(17)-C(16)-C(15)	109.90(18)
N(17)-C(16)-H(16A)	109.7	C(15)-C(16)-H(16A)	109.7
N(17)-C(16)-H(16B)	109.7	C(15)-C(16)-H(16B)	109.7
H(16A)-C(16)-H(16B)	108.2	C(17)-N(17)-C(16)	112.44(19)
C(17)-N(17)-C(9)	113.0(2)	C(16)-N(17)-C(9)	113.30(17)
C(17)-N(17)-H(17)	105.7	C(16)-N(17)-H(17)	105.7
C(9)-N(17)-H(17)	105.7	N(17)-C(17)-H(17A)	109.5
N(17)-C(17)-H(17B)	109.5	H(17A)-C(17)-H(17B)	109.5
N(17)-C(17)-H(17C)	109.5	H(17A)-C(17)-H(17C)	109.5
H(17B)-C(17)-H(17C)	109.5	C(19)-N(18)-C(3)	127.06(18)
C(19)-N(18)-H(18)	116.5	C(3)-N(18)-H(18)	116.5

Table S13. (continued)

O(19)-C(19)-O(20)	124.6(2)	O(19)-C(19)-N(18)	125.7(2)
O(20)-C(19)-N(18)	109.69(19)	C(19)-O(20)-C(21)	120.47(18)
O(20)-C(21)-C(22)	110.5(2)	O(20)-C(21)-C(23)	101.6(2)
C(22)-C(21)-C(23)	110.7(3)	O(20)-C(21)-C(24)	109.7(2)
C(22)-C(21)-C(24)	112.5(3)	C(23)-C(21)-C(24)	111.4(3)
C(21)-C(22)-H(22A)	109.5	C(21)-C(22)-H(22B)	109.5
H(22A)-C(22)-H(22B)	109.5	C(21)-C(22)-H(22C)	109.5
H(22A)-C(22)-H(22C)	109.5	H(22B)-C(22)-H(22C)	109.5
C(21)-C(23)-H(23A)	109.5	C(21)-C(23)-H(23B)	109.5
H(23A)-C(23)-H(23B)	109.5	C(21)-C(23)-H(23C)	109.5
H(23A)-C(23)-H(23C)	109.5	H(23B)-C(23)-H(23C)	109.5
C(21)-C(24)-H(24A)	109.5	C(21)-C(24)-H(24B)	109.5
H(24A)-C(24)-H(24B)	109.5	C(21)-C(24)-H(24C)	109.5
H(24A)-C(24)-H(24C)	109.5	H(24B)-C(24)-H(24C)	109.5
C(26)-N(25)-C(6)	120.6(2)	C(26)-N(25)-H(25)	119.7
C(6)-N(25)-H(25)	119.7	O(26)-C(26)-N(25)	121.2(2)
O(26)-C(26)-C(27)	122.2(2)	N(25)-C(26)-C(27)	116.7(2)
C(26)-C(27)-H(27A)	109.5	C(26)-C(27)-H(27B)	109.5
H(27A)-C(27)-H(27B)	109.5	C(26)-C(27)-H(27C)	109.5
H(27A)-C(27)-H(27C)	109.5	H(27B)-C(27)-H(27C)	109.5
C(2S)-C(1S)-H(1S)	109.5	C(2S)-C(1S)-H(2S)	109.5
H(1S)-C(1S)-H(2S)	109.5	C(2S)-C(1S)-H(3S)	109.5
H(1S)-C(1S)-H(3S)	109.5	H(2S)-C(1S)-H(3S)	109.5
O(3S)-C(2S)-C(1S)	111.5(3)	O(3S)-C(2S)-H(4S)	109.3
C(1S)-C(2S)-H(4S)	109.3	O(3S)-C(2S)-H(5S)	109.3
C(1S)-C(2S)-H(5S)	109.3	H(4S)-C(2S)-H(5S)	108.0
C(2S)-O(3S)-H(6S)	114(3)		

Table S14. Anisotropic displacement parameters ($Å^2 x\ 10^3$) for **20**. The anisotropic displacement factor exponent takes the form: $-2\pi^2[h^2 a^{*2} U^{11} + ... + 2\ h\ k\ a^*\ b^*\ U^{12}]$

	U^{11}	U^{22}	U^{33}	U^{23}	U^{13}	U^{12}
C(1)	29(1)	40(1)	32(1)	-8(1)	8(1)	-10(1)
C(2)	28(1)	43(1)	27(1)	-3(1)	11(1)	-5(1)
C(3)	28(1)	34(1)	21(1)	-2(1)	8(1)	1(1)
O(4)	30(1)	46(1)	24(1)	-8(1)	5(1)	-10(1)
C(4)	24(1)	29(1)	22(1)	0(1)	2(1)	-2(1)
C(5)	24(1)	33(1)	31(1)	2(1)	9(1)	-3(1)
C(6)	35(1)	29(1)	38(1)	4(1)	13(1)	-1(1)
C(7)	52(2)	35(1)	35(1)	10(1)	14(1)	7(1)
C(8)	42(1)	36(1)	23(1)	3(1)	7(1)	8(1)
C(9)	36(1)	33(1)	23(1)	-2(1)	9(1)	1(1)
C(10)	35(1)	44(1)	30(1)	-12(1)	9(1)	-9(1)
C(11)	29(1)	34(1)	24(1)	-3(1)	8(1)	-3(1)
C(12)	23(1)	30(1)	20(1)	-1(1)	6(1)	-1(1)
C(13)	22(1)	31(1)	23(1)	1(1)	7(1)	-1(1)
C(14)	30(1)	31(1)	23(1)	2(1)	10(1)	3(1)
C(15)	27(1)	35(1)	28(1)	3(1)	8(1)	4(1)
C(16)	44(1)	36(1)	26(1)	7(1)	11(1)	7(1)
N(17)	45(1)	29(1)	29(1)	1(1)	15(1)	2(1)
C(17)	75(2)	31(1)	42(2)	-2(1)	19(1)	-1(1)
N(18)	25(1)	44(1)	22(1)	-5(1)	8(1)	5(1)
O(19)	29(1)	70(1)	26(1)	-6(1)	3(1)	10(1)
C(19)	33(1)	44(1)	24(1)	-3(1)	8(1)	5(1)
O(20)	32(1)	65(1)	23(1)	-10(1)	6(1)	8(1)
C(21)	39(2)	68(2)	21(1)	-14(1)	4(1)	1(1)
C(22)	54(2)	78(2)	53(2)	-25(2)	13(1)	-11(2)
C(23)	51(2)	86(2)	32(1)	-19(1)	13(1)	5(2)
C(24)	53(2)	86(2)	27(1)	0(1)	4(1)	12(2)
N(25)	31(1)	32(1)	38(1)	-2(1)	7(1)	-1(1)
O(26)	51(1)	57(1)	65(1)	-25(1)	18(1)	-21(1)
C(26)	44(2)	33(1)	45(1)	-6(1)	13(1)	-3(1)
C(27)	52(2)	56(2)	63(2)	-18(2)	22(2)	6(1)
C(1S)	75(2)	50(2)	66(2)	-5(2)	39(2)	-2(2)
C(2S)	47(2)	86(2)	35(2)	-11(1)	12(1)	13(2)
O(3S)	33(1)	77(2)	43(1)	-25(1)	12(1)	-2(1)
Cl(28)	38(1)	80(1)	29(1)	4(1)	11(1)	14(1)

Table S15. Hydrogen coordinates (x 10^4) and isotropic displacement parameters (Å^{2}x 10^3) for **20**

	x	y	z	U(eq)
H(1)	8461	8543	8328	40
H(2)	8598	7554	7297	38
H(4)	5820(20)	5630(40)	6482(8)	51
H(5A)	4465	5467	8165	35
H(5B)	4938	5180	7543	35
H(6)	5160	3416	8402	40
H(7A)	5392	4487	9449	48
H(7B)	6365	3765	9485	48
H(8A)	7029	5803	9272	41
H(8B)	6579	6033	9915	41
H(9)	6389	8450	9713	36
H(10A)	7317	9414	8952	44
H(10B)	7672	8054	9372	44
H(14)	5218	6958	9129	33
H(15A)	4743	7787	7329	36
H(15B)	4292	7735	7978	36
H(16A)	5773	9478	7864	42
H(16B)	4740	9943	7862	42
H(17)	4970	9194	9004	40
H(17A)	6301	11105	8866	73
H(17B)	6070	10795	9597	73
H(17C)	5276	11384	8950	73
H(18)	8056	5667	6483	36
H(22A)	6407	3269	4824	93
H(22B)	5843	3771	4057	93
H(22C)	5587	4353	4738	93
H(23A)	8008	5476	4310	84
H(23B)	7294	4508	3776	84
H(23C)	7880	3946	4524	84
H(24A)	5826	6701	4471	85
H(24B)	6084	6338	3756	85
H(24C)	6798	7188	4354	85
H(25)	6955	4038	8407	40
H(27A)	7159	1678	7356	84
H(27B)	7637	3057	7690	84
H(27C)	6986	3034	6900	84
H(1S)	5960	9517	6488	90
H(2S)	5581	8848	5727	90
H(3S)	5114	8465	6344	90
H(4S)	5042	11069	5750	67
H(5S)	4203	10005	5533	67
H(6S)	4730(20)	11320(30)	6747(18)	76

Table S16. Torsion angles [°] for **20**

C(11)-C(1)-C(2)-C(3)	1.4(4)	C(1)-C(2)-C(3)-C(4)	-0.2(4)
C(1)-C(2)-C(3)-N(18)	-176.8(2)	C(2)-C(3)-C(4)-O(4)	178.6(2)
N(18)-C(3)-C(4)-O(4)	-5.1(3)	C(2)-C(3)-C(4)-C(12)	-2.8(3)
N(18)-C(3)-C(4)-C(12)	173.5(2)	C(13)-C(5)-C(6)-N(25)	-73.4(2)
C(13)-C(5)-C(6)-C(7)	51.7(3)	N(25)-C(6)-C(7)-C(8)	76.8(3)
C(5)-C(6)-C(7)-C(8)	-49.2(3)	C(6)-C(7)-C(8)-C(14)	53.6(3)
C(14)-C(9)-C(10)-C(11)	37.1(3)	N(17)-C(9)-C(10)-C(11)	-83.6(3)
C(2)-C(1)-C(11)-C(12)	0.4(4)	C(2)-C(1)-C(11)-C(10)	-179.9(2)
C(9)-C(10)-C(11)-C(1)	172.2(2)	C(9)-C(10)-C(11)-C(12)	-8.0(4)
C(1)-C(11)-C(12)-C(4)	-3.2(3)	C(10)-C(11)-C(12)-C(4)	177.0(2)
C(1)-C(11)-C(12)-C(13)	-177.2(2)	C(10)-C(11)-C(12)-C(13)	3.0(3)
O(4)-C(4)-C(12)-C(11)	-176.84(19)	C(3)-C(4)-C(12)-C(11)	4.4(3)
O(4)-C(4)-C(12)-C(13)	-3.1(3)	C(3)-C(4)-C(12)-C(13)	178.2(2)
C(6)-C(5)-C(13)-C(15)	-169.59(18)	C(6)-C(5)-C(13)-C(14)	-54.8(2)
C(6)-C(5)-C(13)-C(12)	68.5(2)	C(11)-C(12)-C(13)-C(15)	89.9(2)
C(4)-C(12)-C(13)-C(15)	-83.9(2)	C(11)-C(12)-C(13)-C(14)	-26.7(3)
C(4)-C(12)-C(13)-C(14)	159.61(19)	C(11)-C(12)-C(13)-C(5)	-147.7(2)
C(4)-C(12)-C(13)-C(5)	38.5(3)	N(17)-C(9)-C(14)-C(8)	-171.74(17)
C(10)-C(9)-C(14)-C(8)	63.9(2)	N(17)-C(9)-C(14)-C(13)	61.9(2)
C(10)-C(9)-C(14)-C(13)	-62.4(2)	C(7)-C(8)-C(14)-C(9)	174.31(19)
C(7)-C(8)-C(14)-C(13)	-60.3(2)	C(15)-C(13)-C(14)-C(9)	-60.0(2)
C(5)-C(13)-C(14)-C(9)	-175.60(18)	C(12)-C(13)-C(14)-C(9)	56.7(2)
C(15)-C(13)-C(14)-C(8)	174.25(19)	C(5)-C(13)-C(14)-C(8)	58.6(2)
C(12)-C(13)-C(14)-C(8)	-69.1(2)	C(14)-C(13)-C(15)-C(16)	55.5(2)
C(5)-C(13)-C(15)-C(16)	169.36(18)	C(12)-C(13)-C(15)-C(16)	-62.9(2)
C(13)-C(15)-C(16)-N(17)	-53.4(3)	C(15)-C(16)-N(17)-C(17)	-175.1(2)
C(15)-C(16)-N(17)-C(9)	55.2(3)	C(14)-C(9)-N(17)-C(17)	171.00(19)
C(10)-C(9)-N(17)-C(17)	-66.9(2)	C(14)-C(9)-N(17)-C(16)	-59.6(2)
C(10)-C(9)-N(17)-C(16)	62.5(2)	C(2)-C(3)-N(18)-C(19)	-139.5(3)
C(4)-C(3)-N(18)-C(19)	44.0(4)	C(3)-N(18)-C(19)-O(19)	-10.3(4)
C(3)-N(18)-C(19)-O(20)	170.7(2)	O(19)-C(19)-O(20)-C(21)	0.3(4)
N(18)-C(19)-O(20)-C(21)	179.4(2)	C(19)-O(20)-C(21)-C(22)	-64.2(3)
C(19)-O(20)-C(21)-C(23)	178.3(3)	C(19)-O(20)-C(21)-C(24)	60.4(3)
C(7)-C(6)-N(25)-C(26)	153.0(2)	C(5)-C(6)-N(25)-C(26)	-81.3(3)
C(6)-N(25)-C(26)-O(26)	-3.6(4)	C(6)-N(25)-C(26)-C(27)	176.1(2)

Table S17. Hydrogen bonds for **20** [Å and °]

D-H...A	d(D-H)	d(H...A)	d(D...A)	<(DHA)
O(4)-H(4)...O(19)	0.822(12)	1.777(16)	2.572(2)	162(4)
C(5)-H(5B)...O(4)	0.99	2.10	2.797(3)	125.6
N(17)-H(17)...Cl(28)	1.00	2.07	3.028(2)	159.4
C(17)-H(17B)...Cl(28)#1	0.98	2.96	3.822(3)	147.7
N(18)-H(18)...O(3S)#2	0.88	1.98	2.804(3)	155.1
O(3S)-H(6S)...O(26)#3	0.822(12)	1.814(13)	2.635(3)	177(4)

Symmetry transformations used to generate equivalent atoms:
#1 -x+1,y,-z+2 #2 x+1/2,y-1/2,z #3 x,y+1,z

Supporting Information References

(1) Torres, O. B.; Jalah, R.; Rice, K. C.; Li, F.; Antoline, J. F.; Iyer, M. R.; Jacobson, A. E.; Boutaghou, M. N.; Alving, C. R.; Matyas, G. R. Characterization and optimization of heroin hapten-BSA conjugates: method development for the synthesis of reproducible hapten-based vaccines. *Anal. Bioanal. Chem.* **2014,** 406, 5927-37.

(2) Jalah, R.; Torres, O. B.; Mayorov, A. V.; Li, F.; Antoline, J. F.; Jacobson, A. E.; Rice, K. C.; Deschamps, J. R.; Beck, Z.; Alving, C. R.; Matyas, G. R. Efficacy, but not antibody titer or affinity, of a heroin hapten conjugate vaccine correlates with increasing hapten densities on tetanus toxoid, but not on CRM197 carriers. *Bioconjug. Chem.* **2015,** 26, 1041-53.

(3) Torres, O. B.; Alving, C. R.; Matyas, G. R. Synthesis of Hapten-Protein Conjugate Vaccines with Reproducible Hapten Densities. *Methods Mol. Biol.* **2016,** 1403, 695-710.

(4) Matyas, G. R.; Mayorov, A. V.; Rice, K. C.; Jacobson, A. E.; Cheng, K.; Iyer, M. R.; Li, F.; Beck, Z.; Janda, K. D.; Alving, C. R. Liposomes containing monophosphoryl lipid A: a potent adjuvant system for inducing antibodies to heroin hapten analogs. *Vaccine* **2013,** 31, 2804-10.

(5) Li, F.; Cheng, K.; Antoline, J. F.; Iyer, M. R.; Matyas, G. R.; Torres, O. B.; Jalah, R.; Beck, Z.; Alving, C. R.; Parrish, D. A.; Deschamps, J. R.; Jacobson, A. E.; Rice, K. C. Synthesis and immunological effects of heroin vaccines. *Org. Biomol. Chem.* **2014,** 12, 7211-32.